CHALMERS
UNIVERSITY OF TECHNOLOGY

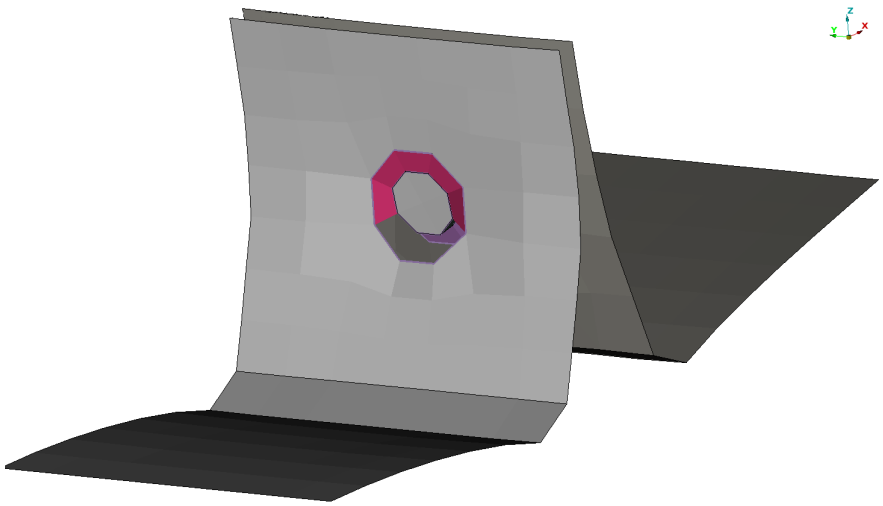

Modeling of Spot Weld with Failure for Crash Simulations

Master's thesis in Automotive Engineering

ADHINATHAN SRINIVASAN RAJALAKSHMI
TISHKO SHAFIQ

Department of Applied Mechanics
CHALMERS UNIVERSITY OF TECHNOLOGY
Gothenburg, Sweden 2017

Master's thesis 2017:49

Modeling of Spot Weld with Failure for Crash Simulations

ADHINATHAN SRINIVASAN RAJALAKSHMI
TISHKO SHAFIQ

CHALMERS
UNIVERSITY OF TECHNOLOGY

Department of Applied Mechanics
Division of Vehicle Safety
Chalmers University of Technology
Gothenburg, Sweden 2017

Modeling of Spot Weld with Failure for Crash Simulations
ADHINATHAN SRINIVASAN RAJALAKSHMI
TISHKO SHAFIQ

Supervisor: Hans Merkle, CEVT AB
Manager: Henrik Tviksta, CEVT AB
Examiner: Robert Thomson, Head of Division Vehicle Safety

Master's Thesis 2017:49
ISSN 1652-8557
Department of Applied Mechanics
Division of Vehicle Safety
Chalmers University of Technology
SE - 412 96, Gothenburg
Sweden
Telephone : +46 (0) 31 772 1000

Department of Applied Mechanics
Gothenburg, Sweden 2017

Modeling of Spot Weld with Failure for Crash Simulations
ADHINATHAN SRINIVASAN RAJALAKSHMI
TISHKO SHAFIQ
Department of Applied Mechanics
Division of Vehicle Safety
Chalmers University of Technology

Abstract

With increasing number of vehicles around the globe, one of the current focus of automotive industry has been vehicle safety. Modern technical advancements in computation field has led to extensive improvements in crash simulation. Spot welds, despite being relatively small in size, contributes hugely to vehicle safety as they hold vehicle body together. The behaviour of spot welds during crash play a vital role and thus, appropriate modelling of spot weld and prediction of failure is essential. Alongside accurate prediction of failure, an added necessity is to save computational time.

The project is carried out in partnership with CEVT AB, where MF GenYld + CrachFEM material model (reference model) is utilised to predict failure of spot weld. The scope of the project is development of a model that reduces computational time, yet achieving results of reference model. In this project, two approaches are dealt with for achieving the aforementioned objective. Three coupon tests (peel, lap shear and u-tension) are taken as standard test to validate the developed models.

One of the approaches is developing a model that represents spot weld as beams. The results for the 5-beam, 8-beam, 9-beam method were varying. The stiffness curve (force-displacement curve) of the model matched reference stiffness curve either for shear or the other two tests. There were no results obtained where the stiffness curve would match for all three coupon tests. No advantageous change in computation time was observed, but carrying an advantage of no added mass to the model. Another approach is modification of the material card to suit the reference model. The material model considered is General Incremental Stress-State dependent Damage Model (GISSMO). The GISSMO material card was developed by another master thesis project and suitability of the model to spot welds is investigated in this project. The approach provided promising results, where the resulting stiffness curve closely represented reference model and also, significant decrease in computational time.

The reference model reproduces damage model on the heat affected zone (HAZ) but not on the actual spot weld. Modelling with beams are valid only when beams represent the reference mesh pattern. The GISSMO model represents reference model closely and it can be used in early modelling stages to save computational time.
Keywords: Crash simulation, material modelling, spot weld modelling, damage model, optimisation, GISSMO, beam

Acknowledgements

Firstly, we would like to thank the company, CEVT AB for providing opportunity to take on the project. There have been many people who have helped in successfully carrying out the project. The deepest appreciation goes to those people. One of them is senior manager of CAE Crash Safety division at CEVT, Henrik Tviksta who has made the master thesis project a possibility and has provided us with all the resources needed to accomplish the project. Special thanks go to the examiner at Chalmers University of Technology, Robert Thomson for the opportunity to guide through the project, for believing us and encouraging us with the work. The sincerest appreciation goes to our supervisor Hans Merkle for the incredible and instrumental effort he has put into the work. He helped us with the project during the whole period and has guided us through our up and downs. It has been a journey of learning and would not been possible without Hans Merkle. Again, thanks for the time and determination put into the project.

Adhinathan Srinivasan Rajalakshmi, Gothenburg, June 2017
Tishko Shafiq, Gothenburg, June 2017

Contents

List of Figures

List of Tables

1
Introduction

This chapter is about the background, purpose and limitation of the project. These areas are explained more methodically.

1.1 Background

The Swedish automotive industry generates over half a million jobs in Sweden, whereas over 130 000 of them are directly employed. 12 percent of Sweden's total export is from the automotive industry, corresponding to over 180 billion Swedish crowns [13]. One important division of the automotive industry is safety. During last decades the demand for safety has increased significantly. The Zero Vision in Sweden, pertaining the aim of the Transport Administration is to have zero death and severe injuries in traffic in Sweden. The decision is established by the Swedish parliament [14].

Simulating vehicle crash scenarios, assist largely in development of safer vehicles. Modern cars are built over monocoque chassis, which are joined together by 4000-5000 spot welds [8]. Current crash simulation software offers a range of ways to model these spot welds. The prediction of the failures in the simulations are of great importance for the safety of the vehicles. If accurate results are produced in early stages of the production then safer vehicles can be manufactured. This project deals with development of a new spot weld modeling technique and using a different material modelling to reduce the computational time.

1.2 Spot welds

Spot welding is a commonly used welding technique in the automotive industry to fuse very thin metal parts to each other. The technique is used to join 2 or more sheets together. Two sheets are placed between the electrodes and high current runs through them. This generates extreme heat on spots where electrodes are in contact with the sheets, see Figure 1.1. The sheets are permanently bonded with a weld nugget, see Figure 1.2, created without effecting remaining material except for very small region around the spot weld. This small region surrounding the weld nugget is a heat affected zone (HAZ), see Figure 1.2.

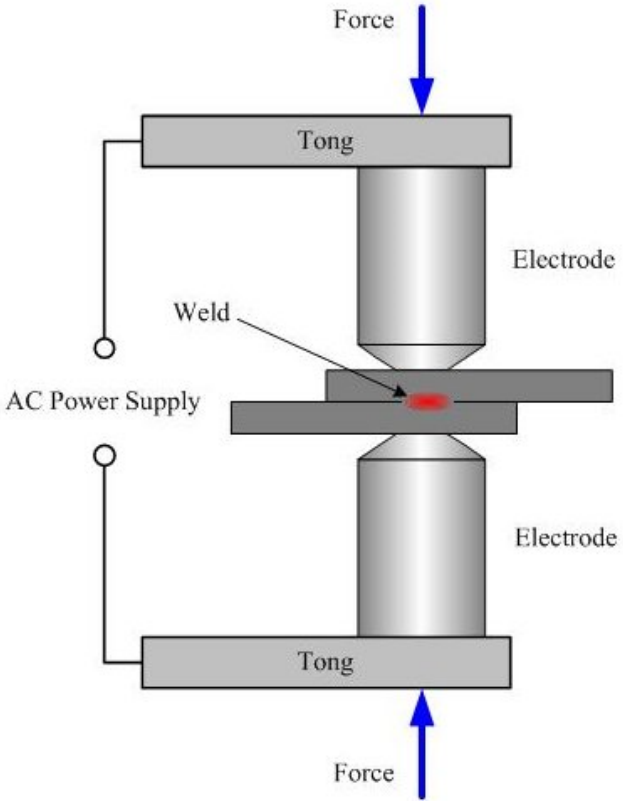

Figure 1.1: Spot welding technique, as seen from side view [16].

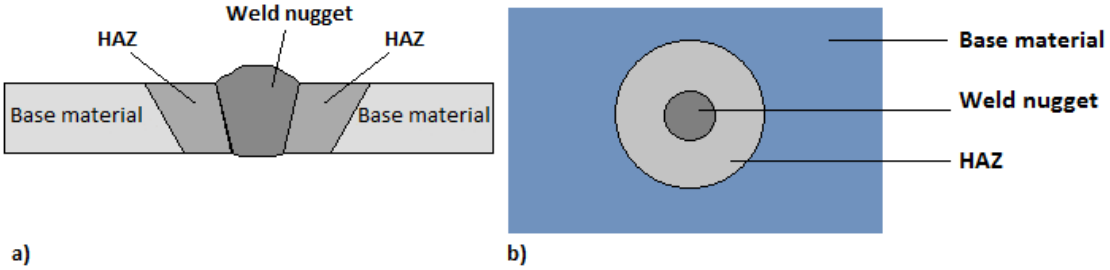

Figure 1.2: The spot weld and the heat affected zone (HAZ). As observed from side view (a) and top view (b).

When the spot welds are exposed to different forces, the bonded sheets can fail, see Figure 1.3, in different ways depending on the exposed load cases. Spot weld failure in a vehicle structure can result in undesirable deformations of the body, which can adversely affect the vehicle safety. Thus, the spot welds play a very vital role in vehicle crash safety. With advancements in computational resources, modelling and simulation plays a important role in vehicle development. In vehicle models for crash safety, the prime demand is towards accurate modelling of spot weld.

In this project, spot welds are simulated with conditions which reflect the load cases during a vehicle crash. During application of such loads, the observations are made on behaviour of a stiffness curves. A traditional way to observe and measure above

mentioned criteria is physical testing. However, simulations are much faster and cost effective compared to physical testing.

Current spot weld modelling techniques are accurate, however, the techniques demand high computational time. Two different ways are explored to bring down computational time, yet retaining the accuracy. One way of obtaining less computational time is by modelling spot welds with beam elements. This method considers alternative modelling of spot weld alone to decrease the computational time. Another method is focuses on alternative material modelling of HAZ region to reduce computational time.

Figure 1.3: Spot weld failure due to peeling [17].

1.3 Purpose

The purpose of the project is to develop a new method in prediction of spot weld failure with the same or almost the same accuracy as the current method but with decreased computational time.

1.4 Objectives

- Developing a new spot weld model by using beams for the nugget and altering the mesh of the HAZ to obtain the same results or almost same results as with the current used model.

- Current material model of spot weld (MF GenYld + CrachFEM) was regarded as time-consuming during simulation of spot weld failure. There is significant saving in simulation time with GISSMO failure type in place of CrachFEM failure type which was observed by another project at CEVT AB [1]. But, the material cards were not tested for compatibility with spot welds. In this project, investigations are done to verify if the method works on spot welds.

1.5 Limitations and Scope

There are many parameters that can be taken into account while developing methods to predict spot weld failure. This project focuses on method development and it is limited in different ways to a single segment, which can be extended to other materials.

- Size of the spot weld. Of the different sizes of spot weld, only 1 size will be investigated. Among various sizes, 4.5 mm spot weld is considered as majority of spot welds in a vehicle's body.

- For the base setup, 3 coupon configurations will be carried out. The configurations are: u-tension, lap-shear and peel.

- Of the different materials in vehicle body, this study investigates on boron steel. This is because a branch of project focuses on material cards developed by Sandberg H., Rydholm O. (2016), which are boron steels.

- The thickness of the sheet metal in the body varies, however 1.4 mm thick sheet metal is studied in the project. This is because 4.5 mm diameter spot welds are predominantly used over 1.4 mm thick sheet metals.

- In the industry the same type of spot weld can have different qualities. The quality of the spot weld is not identical for same type of physical spot weld, one spot weld and differ from another spot weld even if they are the same size and done by the same machine. They can differ in strength and stiffness. However, in this project it is assumed that same type of spot welds have the same qualities due to lack of statistical data.

- Physical tests are not carried out for this project.

2
Literature study

This section details the literature studies that has been carried out to understand various approaches of modelling of spot weld with failure and testing the spot weld models. Some of the suitable approaches are detailed in this section.

2.1 Spot weld properties

A study from Lim et al., 2015 focuses on comparing experimental data with results obtained from modeling of spot weld with finite element method. The physical experiments comprised of coupon tests: tension, with angled tension of 30 degrees and 45 degrees, 60 degrees, lap shear, pure shear and peel. The article provides useful information about coupon testing of spot weld specimen.

A function describing normal failure load, the shear failure load and the failure moment of a spot weld was used to model the spot weld with failure. The aforementioned tests are observed to have influence on the spot weld except for torsion, which was not common in the automotive body structures. With the same function, force-displacement curves for the modelled spot weld are matched to the experimental data with the least square method, see Figure 2.1 [4]. The function was used along with spot weld failure assessment system (SWFAS) program to predict the failure. The matching of curves were well and the method was recommended to be used together with SWFAS program.

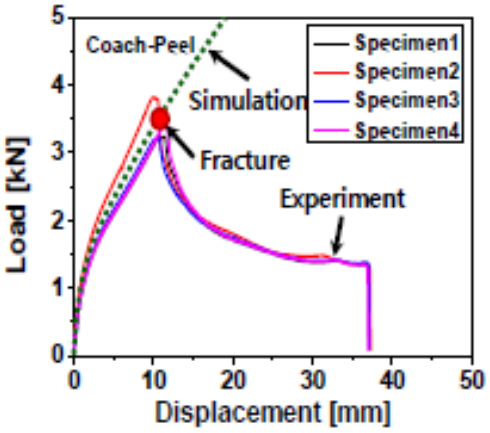

Figure 2.1: The results of the force displacement curves for coach-peel test [4].

2.2 Material definition for spot weld

The approach by Koralla et al., 2015 used LS-Dyna's MAT_240 for the predicting spot weld failure. MAT_240 is a rate-dependent, elastic-ideally plastic cohesive zone model. The specimen tests were similar to study [4] described in Section 2.1. Figure 2.2 shows the various coupon tests including the angled tensile tests.

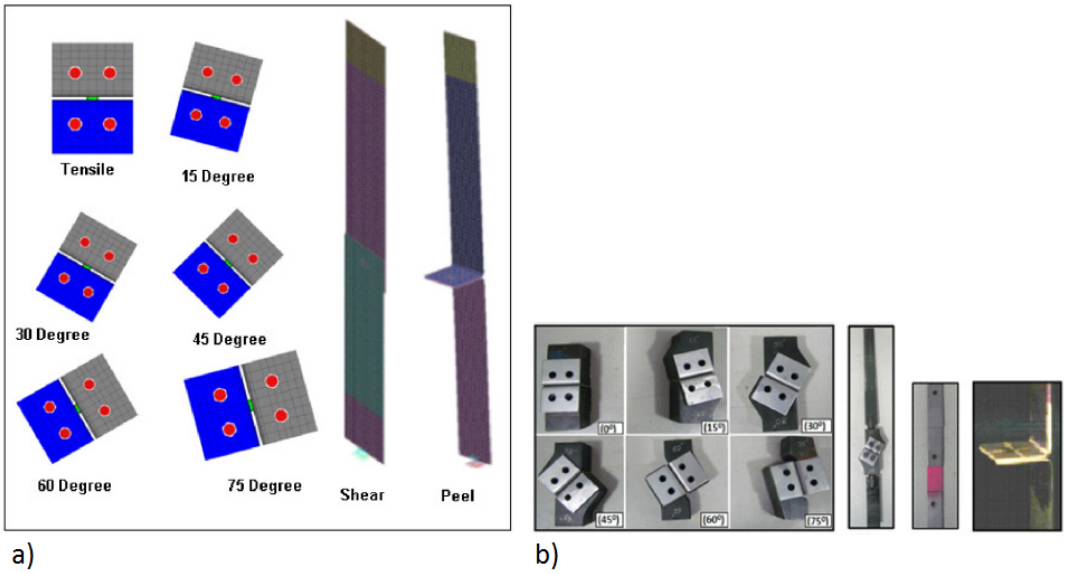

Figure 2.2: The coupons tests a)in the simulations b) physical experiments [5].

The simulation outcome were compared with experimental data and the results were promising according to the study [5]. The method with MAT_240 showed good results when tested in BIW and full vehicle level, see Figure 2.4.

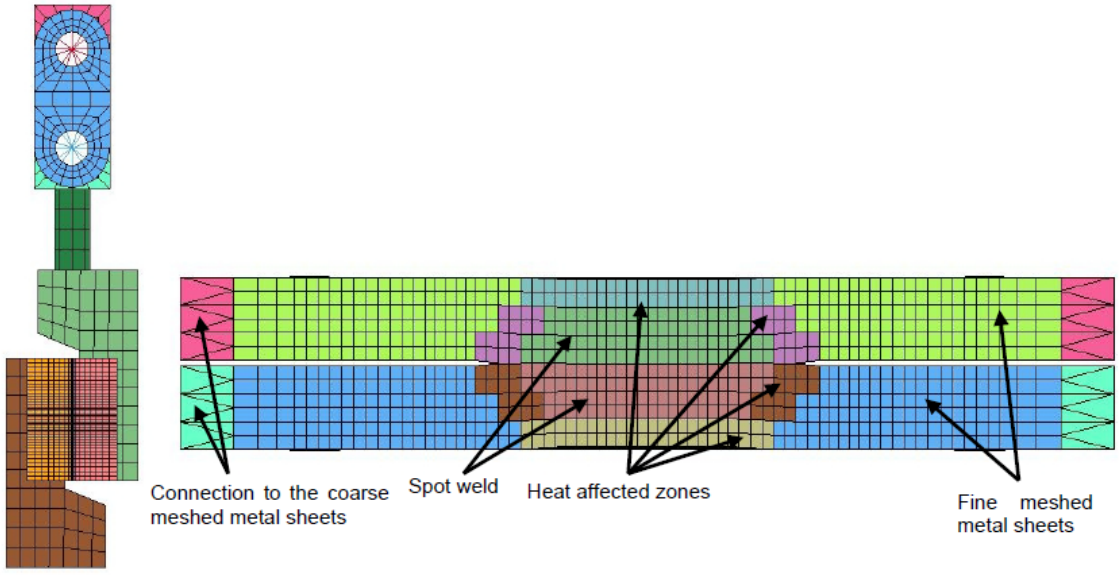

Figure 2.3: Detailed meshing of the spot weld and the surrounding [6].

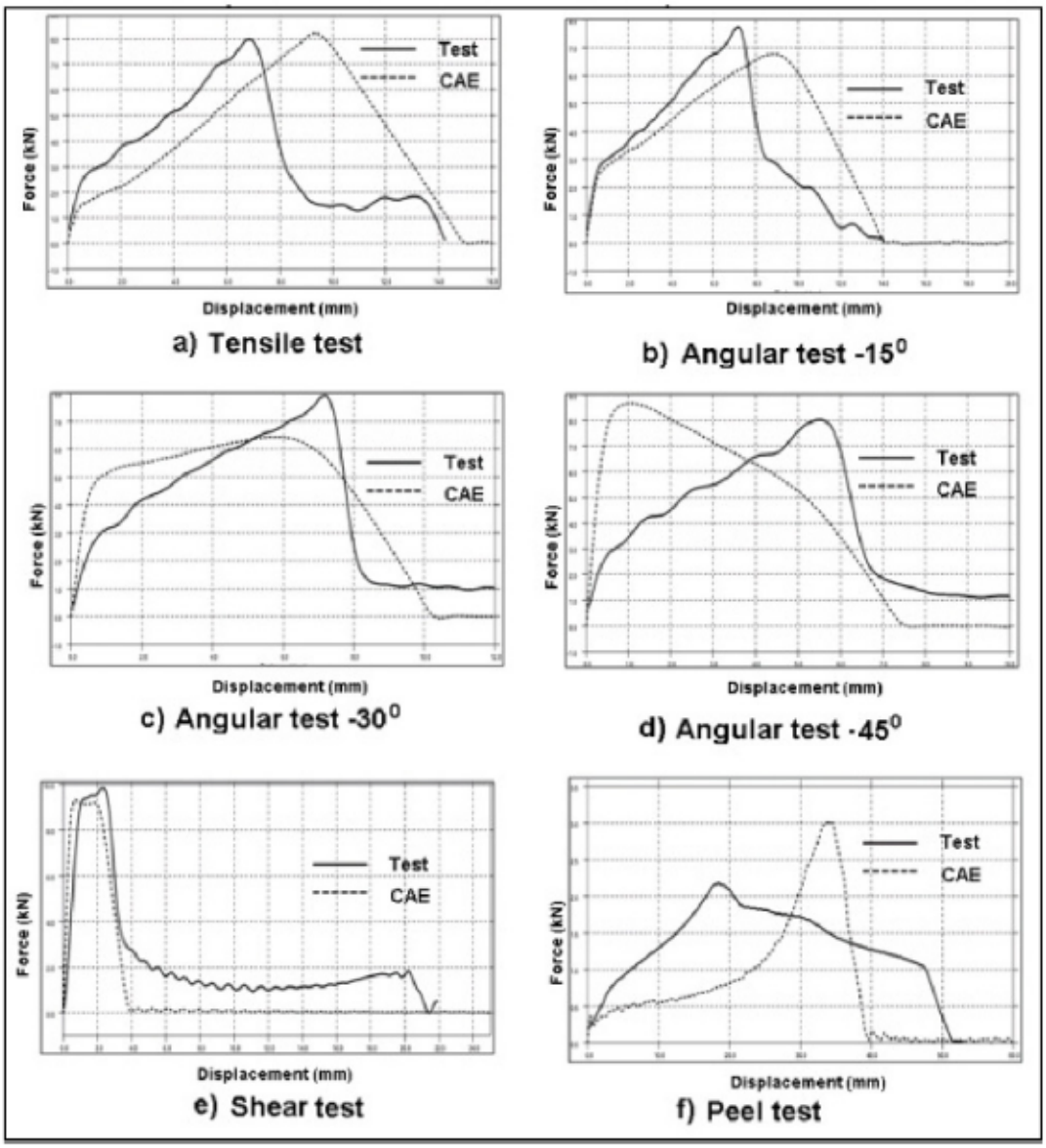

Figure 2.4: The results for coupons tests, both in simulation and experimental [5].

To completely understand the behaviour of the spot weld failure, detailed meshing of spot weld and HAZ region were used by Bier et al., 2015. The detailed meshing of the specimen is shown in Figure 2.3. This method had good accuracy and showed that the failure of the spot was dependent on the material around the spot weld. However, it was very computational costly and can consequently not be used in crash simulations [6].

2.3 HAZ detailed modeling

In the study [7], the main focus was on the HAZ and its effect on the failure of the spot weld. DP980 steel sheet of 1.2 mm thickness was used. The spot weld modelling was very specific with detailed welding parameters and the HAZ was divided into different zones, as shown in Figure 2.5.

The study [7] focused on temperature levels in the sub-critical area, as it was assumed that DP steel was temperature dependent. In the simulation a very fine mesh for the structure was used as shown in Figure 2.6. Analysis of the material structure in upper-critical, sub-critical areas and spot weld nugget was investigated throughout the project. Hardness was observed in these areas by micro hardness indentations. The observations from physical experiments made on the critical areas was matching with the simulations [7].

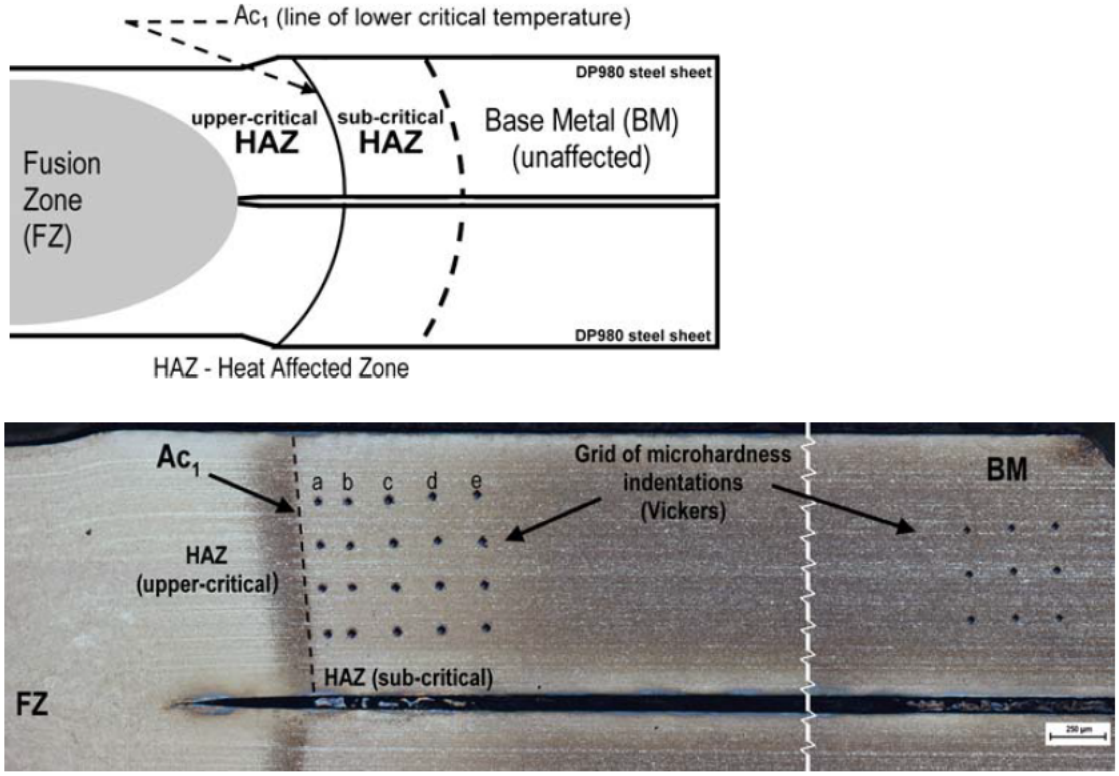

Figure 2.5: The critical areas of the spot weld [7].

2.4 Modeling of spot weld using springs

A method for predicting spot weld failure using spring elements was published by engineers at Ford Motors [2]. A two-node spring element with 6 degrees of freedom was used as shown in Figure 2.7. The separation of the spot weld was modelled with levels of peak force, displacement and energy.

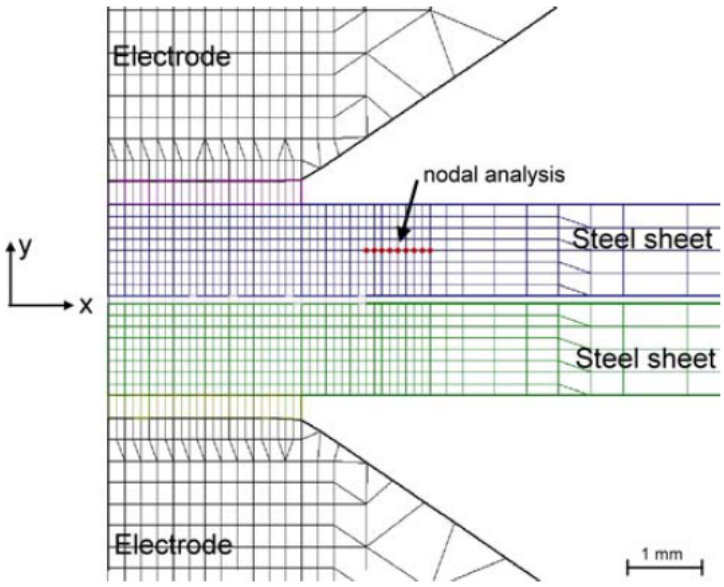

Figure 2.6: The side view of spot weld with base material in the simulation [7].

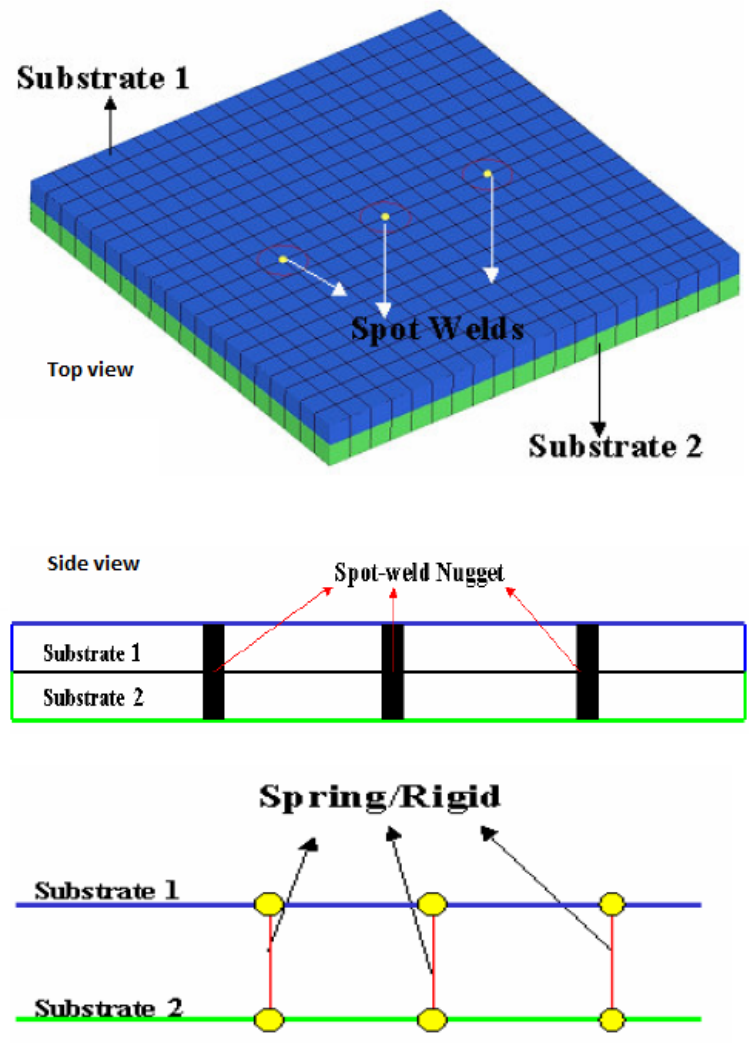

Figure 2.7: Spot weld model using spring elements, top and side view [2].

The model was validated with experimental component tests and compared to CAE simulations. A coupled energy based rupture criterion was used to get good results with reality. The comparison between experimental and simulation results were unstable. Good correlation were achieved in some tests, but also resulted in significant differences with others tests.

2.5 Material Modelling

In the study [1], the traditional material model (MF GenYld + CrachFEM) was replaced with alternative material model (MAT024 + GISSMO). Unlike MF GenYld + CrachFEM, the MAT024 + GISSMO were not encrypted. Therefore, GISSMO material can be modified and used anytime. The definition of the materials are implemented directly in the material card.

Added to non-encrypted format, the simulation with GISSMO material in place of CrachFEM material was much faster in the simulation time, therefore the GISSMO is more desirable [1]. The reason why it has not been implemented was because there has not been any conversion of materials from CrachFEM to GISSMO until the study carried out in 2016. [1].

GISSMO was implemented into the master *.key file in 2 ways. One way was to define the material parameters in the pre-processor. The second method was through including a *.k file for GISSMO material in the master key file. The GISSMO material card contained the data defined by the project carried out earlier [1].

2.6 Summary of literature study

There are clearly many approaches to develop the method to predict spot weld failure. The amount of variables involved, as observed from the aforementioned literature are many. A short summary of the different vital parts to focus on are:

- Material characteristics for spot weld nugget, HAZ and the base material.
- Meshing of HAZ and base material.
- Modelling of spot weld nugget as beams (or) solids (or) springs with appropriate equations.

3
Theory

In this chapter, the prime section of Finite Element Modelling concerned to this project is briefly explained. Furthermore, the theory section also details on material modelling used in the project.

3.1 Finite Element Modelling

3.1.1 Mesh

Meshing is one of the central part of finite element method. Guidelines and techniques exist on how to mesh for different occasions and model setup, but there are not any rules. "All finite elements are based on rather polynomial interpolations of the unknown function within the element" [10]. The smaller the mesh size is, the more accurate the results are. This basically means that interpolations are done to be as close as possible to the actual results. Therefore, smaller mesh sizes results in smaller elements, which in turn gives more accurate results until mesh independence is reached.

However, there is a trade-off between using small mesh sizes and the computational power it demands. In general, the critical parts are given finer mesh and less finer mesh for the non-critical areas. The start can be with a simple FE model and depending on the problem, proceed to a finer mesh if required, see Figure 3.1 [10]. The size of the dimensions of the element are also important to consider. The ratio between the largest and smallest dimension within an element should be 1:1 or as close as possible to obtain a good mesh [10].

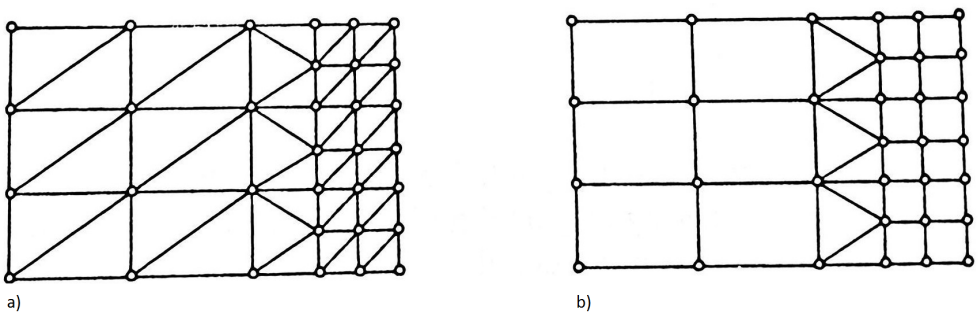

Figure 3.1: In the model, critical area lies on the right side and thus, finer in that area [10]. The mesh has been refined from a to b.

3.1.2 Beams

A beam is shown in Figure 3.2. Some assumptions are made when performing finite element (FE) formulations on beams. This is done to simplify the approach. "The material and cross-section of the beam are assumed to be symmetric about the xz-plane...", see Figure 3.2. Only loading on the xy-plane is taking into account.

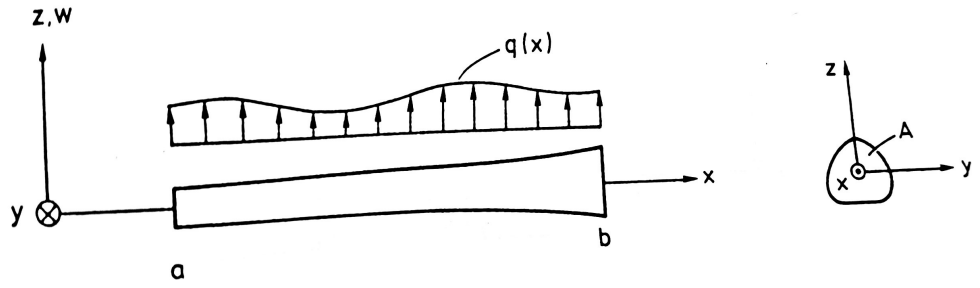

Figure 3.2: The setup of a beam with load q [N/m] [10].

For the beam there is equilibrium conditions which can be calculated when a infinitesimal part of the beam is scrutinized, see Figure 3.3.

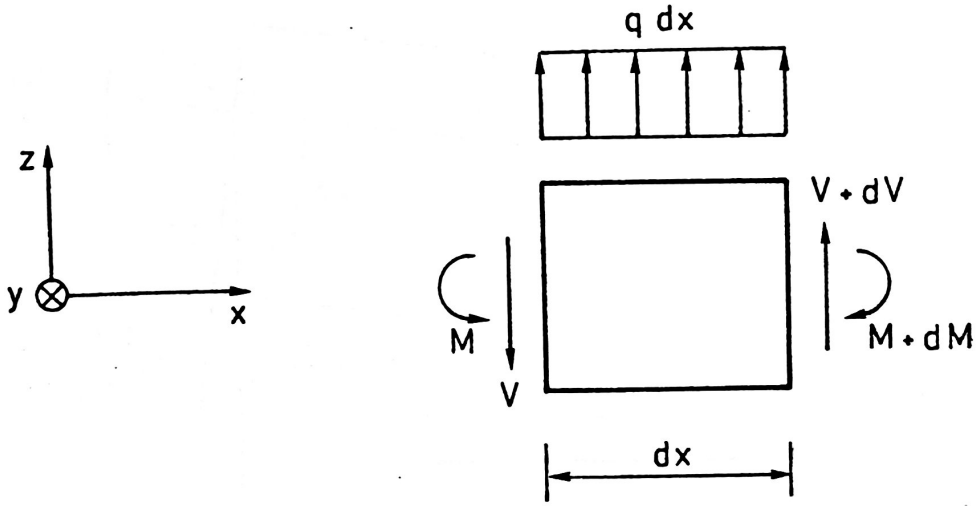

Figure 3.3: Infinitesimal part of a beam [10].

When FE analysis with beams are performed, there are other assumptions in the kinematics and the Bernoulli's assumption are implemented. The Bernoulli's assumption is expressed as: "Plane sections normal to the beam axis remain plane and normal to the beam axis during the deformation". Furthermore linear elasticity is assumed for the beams according to Hooke's law for isotropic material.

3.1.3 Shells

There are many different types of shell formulation techniques handled by LS-Dyna. The shell formulation in LS-Dyna can be ranked in 2 ways - Accuracy and Robustness.

Robustness denotes ability of shell element to be stable in situations like poor element shape and abnormal deformations. Type 2 element, despite being under integrated, when used with Hourglass control type 4, stiffens the element and is recommended by Dyna Support [18].

From accuracy standpoint, shell element type 16 is preferred, but type 16 demands 2.5 times more computational power than type 2. When the shell element 16 is combined with Hourglass control type 8, will give accurate solution for warped geometries. This combination is used for modelling HAZ elements [18].

3.1.4 Mass scaling

In order to obtain larger time step, non-physical mass is added to the model. This techniques is called mass scaling. The physics behind the mass scaling can be explained by using propagation of waves (Stress/Shock) through the model. In the simulation, the time step is calculated by considering the smallest element dimension. By using Courant condition (Equation 3.1, the smallest time step can be calculated.

$$\Delta t \leq f * \left[\frac{h}{c}\right]_{min} \tag{3.1}$$

$$c = \sqrt{\frac{E}{\rho}} \tag{3.2}$$

Where,
Δt is time step,
f is scale factor for stability (usually 0.9),
h is the smallest length in the model,
c is speed of the wave,
E is Young's modulus,
ρ is density.

To increase the time step, three parameters can be altered - element size, Young's modulus and density. In this project, Young's modulus is altered when using solid elements for nugget. Though it carries an advantage of reduced simulation time, this technique can significantly increase the mass of the model. Validation of the technique is necessary and is performed by checking the increase of overall mass of the model.

3.2 Material Modelling

3.2.1 CrachFEM

MF GenYld + CrachFEM is a material model with failure prediction characteristics. The models are encrypted and can be used with commercial finite element software. The MF GenYld uses von Mises yield criterion and isotropic hardening for normal steel materials. An alteration is introduced for rolled steels, where anisotropic criteria are used.

CrachFEM is the module which describes material failure based on two different failure criterion. Ductile normal fracture and ductile shear fracture being the two categories describing the failure for 2D and 3D elements. For shell elements, in addition to the above two categories, a third one is implemented to describe localised necking phenomenon of sheets [15]. The failure criterion are evaluated individually and does not affect each other. Figure 3.4 shows representations of the above mentioned categories.

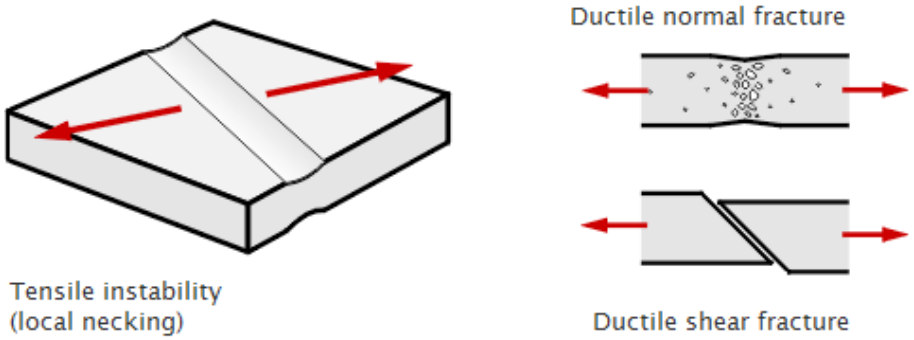

Figure 3.4: Representation of failure mechanisms in CrachFEM module [15].

CrachFEM failure mechanisms take the equivalent plastic strain (measure of the amount of permanent strain) and plastic strain to failure (the accumulated permanent strain at failure) to compute fracture as represented in Equation 3.3. The fracture risk, ψ is defined by the above mentioned values, equivalent plastic strain ϵ_M and plastic strain to failure ϵ_M^*.

$$\psi = \frac{\epsilon_M}{\epsilon_M^*} \tag{3.3}$$

The ductile normal fracture criteria, the equivalent plastic strain at failure depending on the triaxiality and strain rate is considered, $\epsilon_M^* (\eta, \dot{\epsilon}^p)$. For ductile shear fracture, the determines the equivalent plastic strain to failure as function of shear stress parameter and plastic strain rate, $\epsilon_M^* (\theta, \dot{\epsilon}^p)$. The tensile instability considers equivalent plastic strain at the onset of fracture risk as function of inplane deviatoric stress ratio, $\epsilon_M^* (\alpha, \dot{\epsilon}^p)$.

3.2.2 *MAT_ADD_EROSION and GISSMO

Many constitutive models in LS-DYNA do not incorporate any erosion or failure criterion [1] [12] . *MAT_ADD_EROSION is a way to implement failure criterion to a constitutive model with and without failure criterion. If added to a model with failure criterion, the *MAT_ADD_EROSION provides an additional failure criterion. Alongside erosion, GISSMO - General Incremental Stress-State dependent Damage Model (detailed in Section 3.2.2.1) or DIEM - Damage Initiation and Evolution Model can be introduced. The most important parameters which defines the *MAT_ADD_EROSION and GISSMO damage models are represented in the Appendix 3.1.

3.2.2.1 Damage Model

When the damage model, IDAM is set to 1, the GISSMO damage criterion is taken into account [12]. The GISSMO model allows for an incremental description of damage accumulation including softening and failure [12]. The incremental value of Damage D is formulated as given below,

$$\Delta D = \frac{DMGEXP \cdot D^{\left(1-\frac{1}{DMGEXP}\right)} \Delta\epsilon_p}{\epsilon_f} \tag{3.4}$$

Where,
D = Damage measure (0≤F≤1)
ϵ_f = Equivalent plastic strain to failure
$\Delta\epsilon_p$ = Equivalent plastic strain increment

A typical failure curve for metals modelled using shell elements look similar to the graph in the Figure 3.5. The focus of the thesis is limited to tensile part of the curve (marked in red box), as the material card obtained from the previous project carries no compression segment of the curve [1].

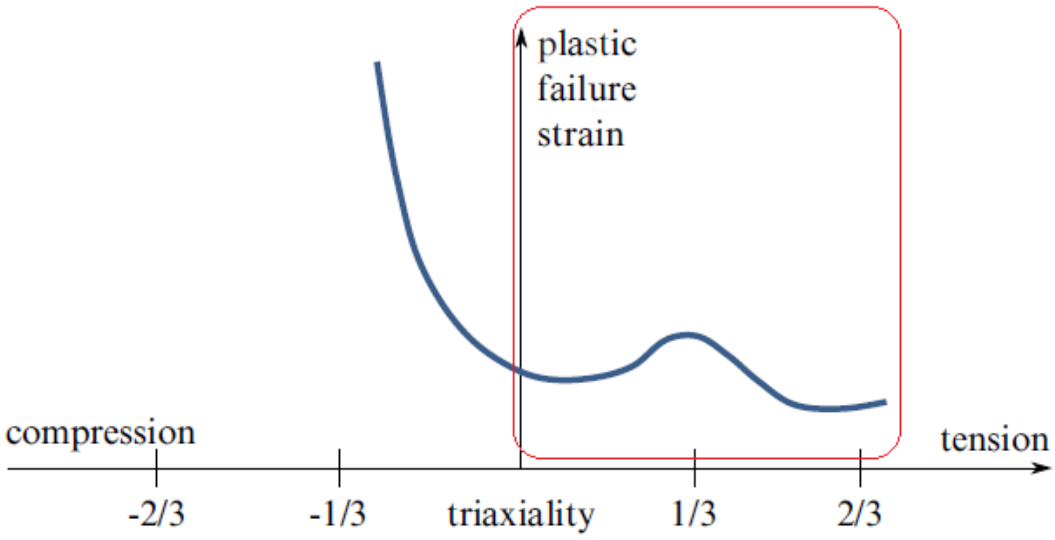

Figure 3.5: Typical failure curve for metals modelled using shell elements [12].

3.2.2.2 Incorporation in LS-DYNA

In LS-DYNA, the *MAT_ADD_EROSION can be included with non-linear element formulations of 2D continuum, 3D solid elements, 3D shell elements and thick shell types 1 and 2 [12]. A number of parameters including the critical parameters mentioned in Table 3.1 are used to describe material properties with erosion and damage.

In this project, *MAT_ADD_EROSION is specified with the *MAT_024 material cards representing boron steel. The *MAT_024 is elasto-plastic constitutive model based on von-Mises yield criterion. The parameters included in the *MAT_024 cars are Young's modulus, Poisson ratio, mass density and load curve defining effective stress against effective plastic strain. A tabular data defining effective stress vs effective plastic strain can be defined for different strain rates. In this project, a strain rate independent material (boron Steel) is considered [1].

The *MAT_024 does not define material behaviour beyond the point of uniform expansion. The *MAT_ADD_EROSION is specified to include that behaviour. The parameters on interest on this segment are IDAM, DMGTYP, LCSDG, ECRIT, DMGEXP, FADEXP (refer Table 3.1). To specify GISSMO damage model within *MAT_ADD_EROSION, the value of IDAM must be set to unity. There are more than one driving quantities signifying the failure of the material. When DMGTYP is set to 1, the digit-wise interpretation happens within LS-DYNA, where value of M is set to 1 and N to 0. With M equal to 1, the flow stress are coupled to damage and element failure occurs when the damage measure (D) reaches unity. With value of N equal to 0, the equivalent plastic strain becomes the driving factor for the damage.

Table 3.1: Significant parameters used in material card

Parameters	Description
IDAM	Indicator for the damage model. IDAM=1 indicates GISSMO damage model.
DMGTYP	Is intepreted digitwise and denotes what type of equations and additional variables will be used to compute damage.
LCSDG	Load curve for triaxiality against equivalent plastic strain at failure
DMGEXP	Exponent for nonlinear coupling of damage. The value is computed by optimization and benchmarking against CrachFEM damage model.
ECRIT	Load curve for triaxiality against critical equivalent plastic strain
FADEXP	Exponent for damage related stress fadeout. The value is computed by optimization and benchmarking against CrachFEM damage model.

4

Methodology

This chapter details on coupon simulations for the reference method, method development for spot welds with beams and method development of the GISSMO material modelling.

4.1 Specimen

For all the methods, three coupon simulations were carried out, which are u-tension test, lap-shear test and peel testing, see Figures 4.1, 4.2 and 4.3. For each coupon test, one sheet was fixed, while the other one had a displacement applied to it which moved the sheet in desired direction. The light blue colored lines parallel to each sheet represents the force carried out on the sheet. The dark blue color indicates that the side is fixed in all degrees of freedom. The coupon tests were baseline for the methods used, see Figure 4.1-4.3.

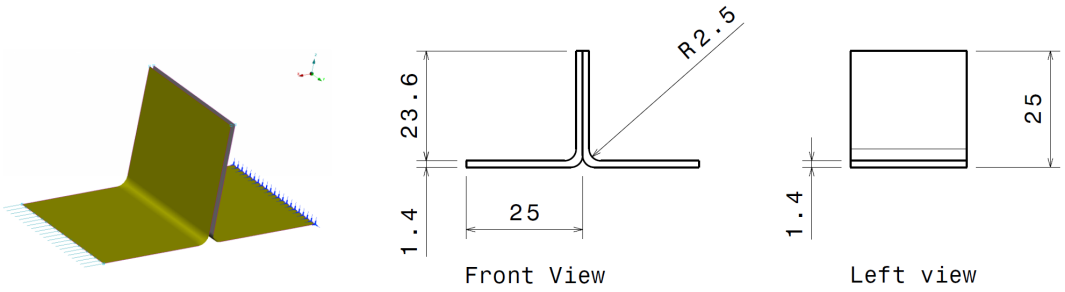

Figure 4.1: The geometry shown is for testing of peel specimen.

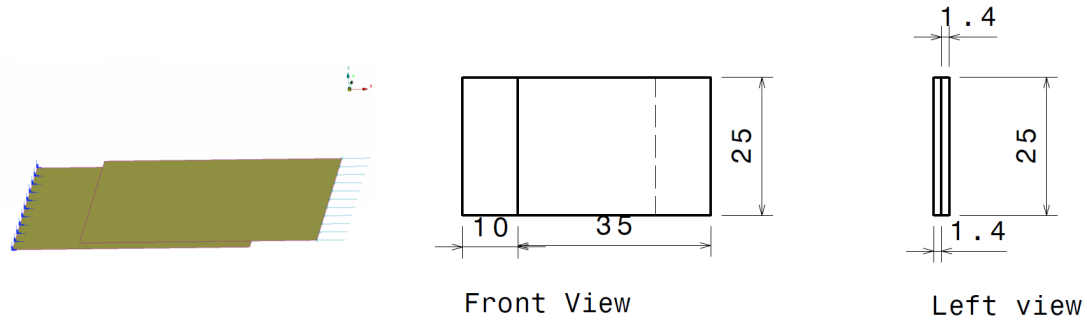

Figure 4.2: The geometry shown is for testing of shear specimen.

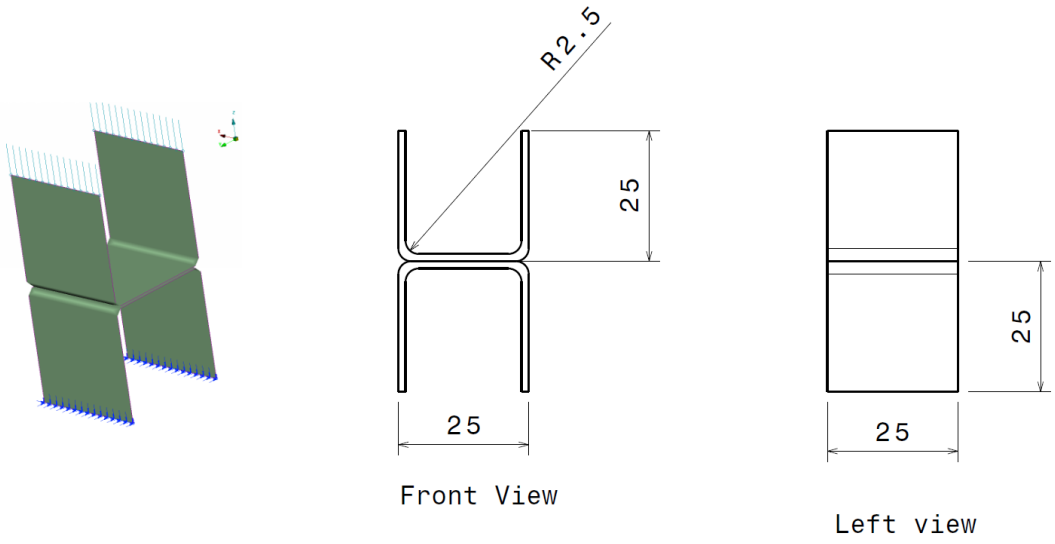

Figure 4.3: The geometry shown is for testing of u-tension specimen.

4.1.1 Reference model

The method for developing a new method for prediction of spot weld failure was carried out by comparing results with the reference model. The reference model, which is currently used at CEVT, is assumed to be very accurate for prediction of spot weld failure. Because of that reason, there were no physical experiment needed to compare results with the reference. The coupon test models were meshed with 3.5 mm sizes.
The units used when simulating was according to Table 4.1 and they are used for the rest of this report.

Table 4.1: Units used in the report.

	Units
Length	millimetre
Time unit	millisecond
Mass unit	kilogramme
Force unit	kiloNewton
Young's modulus of steel	210
Density of steel	7.85E-6
Yield stress of mild steel	0.200
Acceleration due to gravity	9.81E-3
Velocity equivalent to 30mph	13.4

The spot weld are realized using scripts in ANSA and can be used for specific materials. This model focuses on the spot weld in two steps. The reference model consists of a solid nugget which has 4 solid elements. The surrounding 8 nodes on a side of spot weld are connected to another 8 nodes creating the HAZ area with 8 shell elements, see Figure 4.4. The base material (BM) is usually a MAT24-material

which is an encrypted material where the properties cannot be read. These dimensions and areas apply for both sides of the sheets. The solid nugget is made out of Material Type 100 (MAT100) [12].

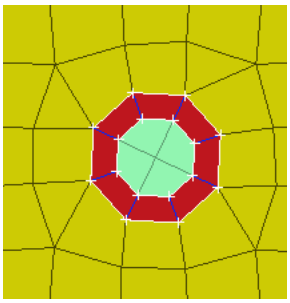

Figure 4.4: Spot weld model. Red colour denotes the HAZ, light green colour denotes nugget and yellow denotes the base material.

4.1.2 Overview

The investigations of the GISSMO method and the development of the new spot weld failure with beams were carried out parallel, see Figure 4.5. When they were done, the idea was to merge the solutions and test the setup together to achieve even better results.

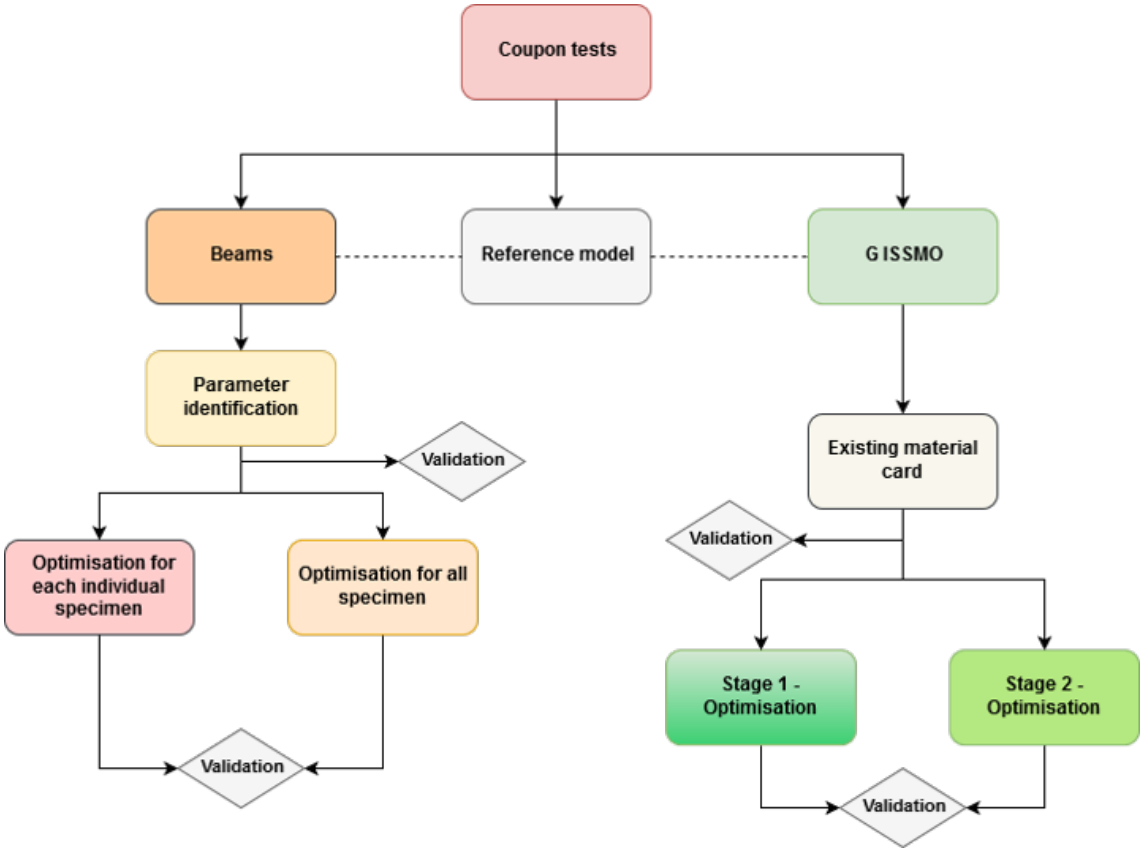

Figure 4.5: The project methodology in steps.

4.2 Beams method

Instead of using a solid nugget as in the case of the reference model, beams will be used to represent the nugget. Initially, a 5-beam method was developed with changes both in the nugget but also in the HAZ. Additionally, 8-beam method along with 9-beam method was developed with changes to the nugget only.

4.2.1 5-Beams method

Instead of using a solid nugget with an 8-element HAZ around it on one layer, as in the reference, the idea was to replace the solid nugget with beams. The size of the solid spot weld was 4.5 mm in diameter which gave the area of 15.9 mm^2, therefore the total area of the beams should be equivalent. There are many ways to setup the beams and the amount of beams are also a variable that can change however 5 beam elements were setup to replace the solid nugget, see Figure 4.6.

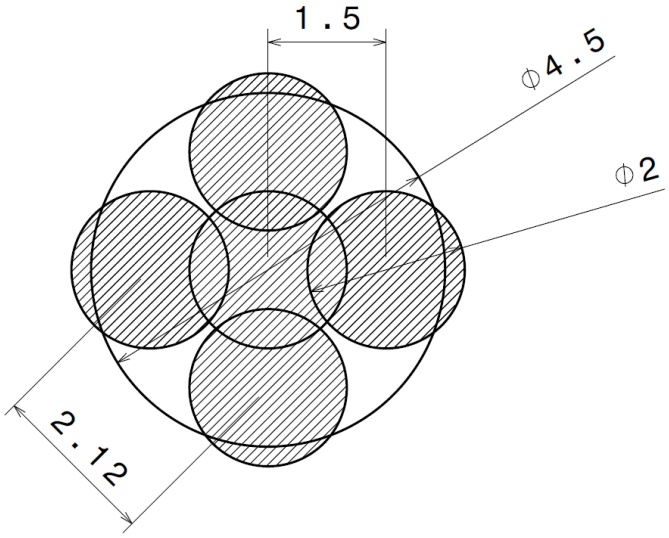

Figure 4.6: The setup of the 5-beam.

4.2.1.1 Setup

The 5-beam method is very similar to the reference model but instead of using a single solid nugget, it has 5 beams (see Figure, 4.7) and a bigger HAZ. The HAZ is generated depending on the position of the beams on the shell elements. Since the element size is bigger in relation to the reference, the HAZ will have a bigger area. The spot weld (in this case, the beams) has an area with HAZ which should be 15.9 mm^2, which is explained in 4.2. In Figure 4.7, the 5-beams are positioned in the zone of 6 shell elements, therefore those elements are assigned as HAZ.

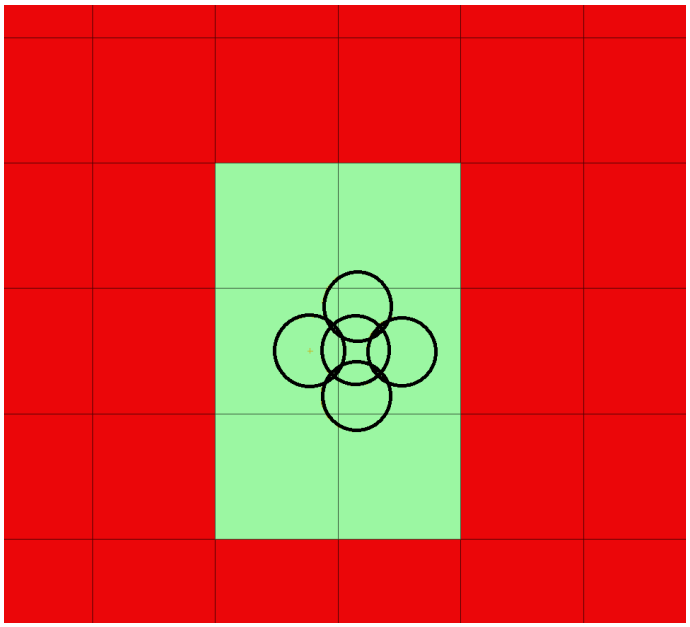

Figure 4.7: The HAZ around a 5-beam spot weld, where the green area is the HAZ and the red BM and the circles represent the beams.

4.2.1.2 Properties

As with the solid nugget, the beams are also made out of MAT100 [12]. Therefore the same material cards are used for the beams. Within the cards, 4 parameters would be changed to fit the force-displacement curves for the 5-beams with the reference model. The 4 parameters are: Ultimate strain (effective plastic strain, EFAIL), initial yield stress (SIGY), young's modulus (E) and the plastic hardening modulus (ET). The positioning of the beams are also of importance. The initial distances between the beams were according to the Figure 4.6.

Table 4.2: Material card 1 for MAT100.

Card 1	1	2	3	4	5	6	7	8
Variable	MID	RO	E	PR	SIGY	ET	DT	TFAIL
Type	555	$7.8*10^3$	X	0.3	X	X	0	0

Table 4.3: Material card 2 for MAT100.

Card 2	1	2	3	4	5	6	7	8
Variable	EFAIL	NRR	NRS	NRT	MRR	MSS	MTT	NF
Type	X	0	0	0	0	0	0	0

4.3 8/9-Beam method

The meshing pattern in the reference specimen was utilised in building a new model with beams. The variations of the beam positioning and mesh types are shown in

Figure 4.8. These variations in model were simulated to check its performance with reference method and carrying an advantage of no added mass. The three variations included,

1. 9-beam
2. 8-beam without central cavity
3. 8-beam with central cavity

4.3.1 Modelling of 9-Beams

The 9-beams were modelled using the connection manager option with ANSA. The shell elements between which the beams are modelled was mentioned within connection manager. Diameter of the beams was formulated by dividing the area of cross section of the representative spot weld with number of beams. In this case, the spot weld in reference model was characterized by a diameter of 4.5mm. The area of cross section (15.9 mm^2) was divided between 9 beams. This gave a resulting diameter of 1.5mm for each spot weld beam.

The beams were realised on 3D spot weld type points. The points were placed over the nodes on the mesh such that the points were nodes of imaginary solid element in the reference model. In that fashion, eight points were placed and the ninth point were placed on the centre of the imaginary solid nugget as in Figure 4.8.

The property definition of beams include element form (9 - Spot weld beam) and outer diameters at either ends of the beam. The material properties of beam were specified in *MAT_100 type including mass density, Young's modulus, Poisson ratio and hardening modulus. The values were same as reference solid nugget except for Young's modulus, which was tested with both 40GPa and 210GPa.

4.3.2 Modelling of 8-Beams

The 8-beams were modelled in the same way as 9-beams in terms of connection between shells, beam properties and material properties. The difference lies in the beam diameter and number of beams. Since, the area of cross section was to be divided between eight beams, the diameter of each beam was set to 1.6 mm. The beams were placed on nodes surrounding the imaginary solid nugget. They were then simulated with 3 variants. One variation was using 40GPa and 210 GPa for Young's modulus. The other variation was having elements in the region between the beams.

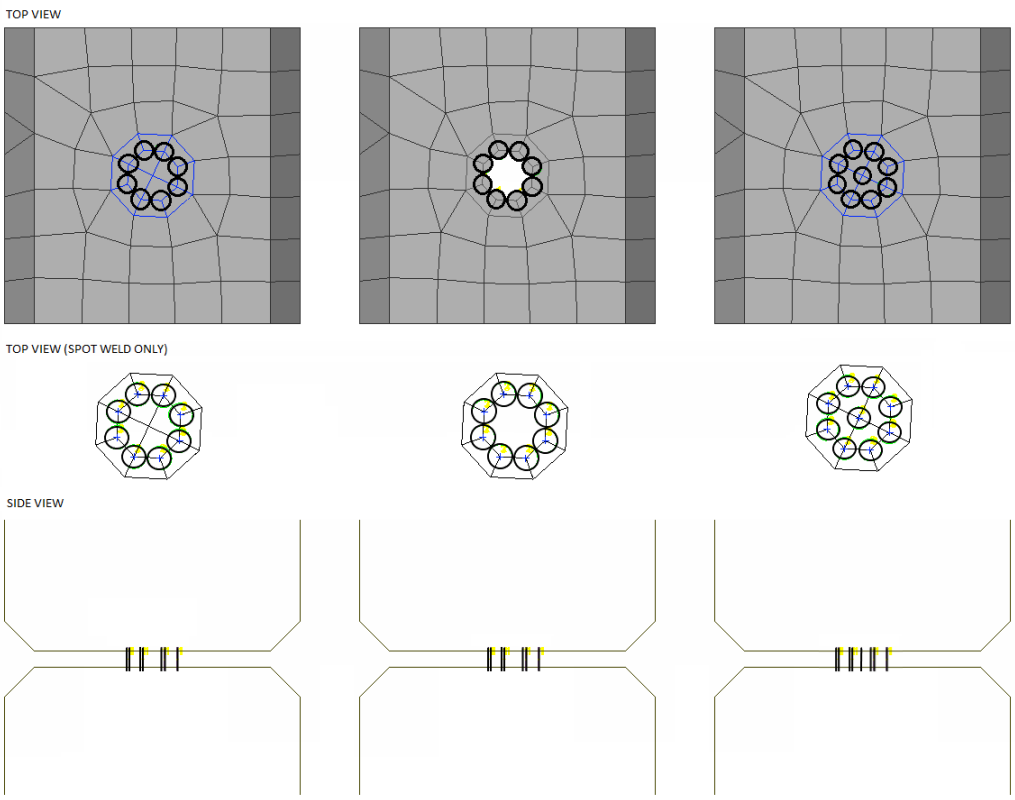

Figure 4.8: Variations in mesh and beams.

4.4 GISSMO Material modelling

The GISSMO material cards from the study [1] were tested to check their compatibility for spot welds. For the test, the material cards were assigned to HAZ region and the results were benchmarked against reference model. The differences were significant and demanded further optimisation of the material card to suit spot welds.

4.4.1 Optimisation of GISSMO material card

4.4.1.1 Modelling

The pre-processing stage includes using the already created coupon test models and defining suitable conditions within master key file. The models used in the optimisation are the same described in the Section 4.1. The master key file was altered to define the parameters and include modified GISSMO material card. The modification performed on the material model was inclusion of the defined parameters and initializing the same.

4.4.1.2 Optimisation

The parameters considered and stage-wise optimisation followed the same pattern as in the study [1]. The steps are detailed as follows,

1. The definition of *MAT_024 comes first with Young's modulus, mass density, Poisson ratio and a curve relating effective stress against effective strain. This can derived from force-displacement curves of standard specimen tested with CrachFEM with appropriate settings including ELFORM, Thickness.
2. The next step being optimisation of DMGEXP and FADEXP. This was done through optimisation of tensile specimen with reference curve being same specimen simulated with CrachFEM .
3. Upon optimisation of DMGEXP and FADEXP, two curves (ECRIT and LCSDG) are optimised against triaxiality ≥ 0 (tensile region). The optimisation is performed with five specimens with reference curves obtained by simulation with CrachFEM.
4. The final step in obtaining the GISSMO material card is optimisation of LCREGD curve. This regularisation curve is obtained upon optimisation of specimens with varying mesh sizes with reference curve of the same specimens with CrachFEM.

4.4.1.3 LS-OPT Setup

Optimisation software, LS-OPT was utilised for optimising of the DMGEXP, FADEXP, ECRIT and LCSDG. The layout of LS-OPT used to optimise the parameters is shown in Figure 4.9.

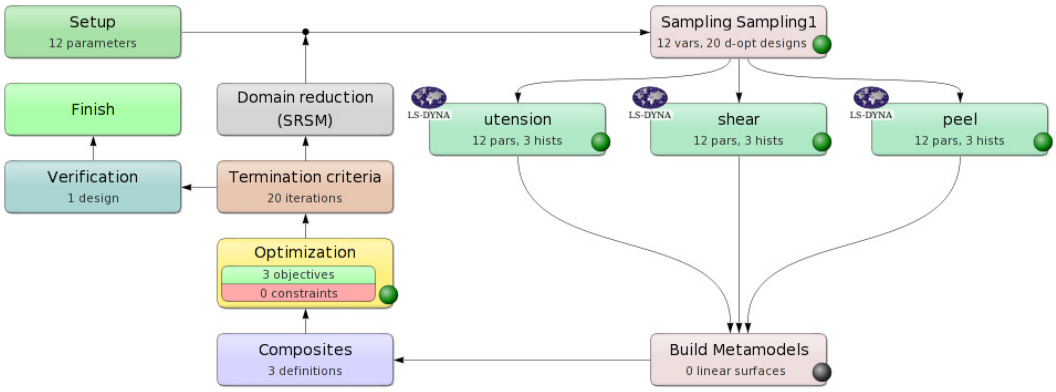

Figure 4.9: Optimisation of GISSMO card curves with coupon specimens

The parameters defined in the master key file were given a range in the 'Setup' box. The models of specimens were selected in the stage, which are then matched against the reference curves. The reference curves were added in the composite block which uses curve mapping algorithm. The optimisation objectives with three curve matching and their weights (one for all the three optimisation objectives) are specified in the 'Optimisation' block. The maximum iterations and convergence stopping criteria are mentioned in the 'Termination Criteria' block.

4.4.2 Variations modelling, if necessary

Upon optimisation of GISSMO cards for coupon test specimens, they are tested for variations in material properties and surrounding mesh size. Some variations involve new models of the same coupon test with updated denser/coarser mesh.

4.4.2.1 Modeling with of many triaxiality points

The ECRIT and LCSDG curve which contain equivalent critical plastic strain and equivalent plastic strain to failure against triaxialities are initially modelled with 6 parameters per curve. This discretisation was changed and parameters in each was increased to 11. The change is defined in the master key file, where the parameters are defined and also, in the GISSMO material card, where the parameters are initialised.

4.4.2.2 Variation of surrounding mesh

The size of the mesh of the solid nugget and the HAZ region changed only with variation in diameter of the spot weld and always remained same irrespective of surrounding mesh size. The Figure 4.10 shows top view of specimens depicting difference in the mesh size for the base material region for the same spot weld diameter for an u-tension specimen.

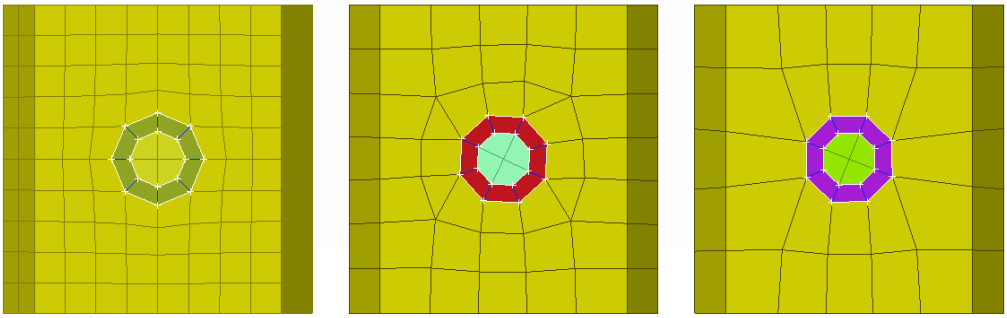

Figure 4.10: Variation in mesh size for base material with 4.5mm diameter spotweld

5
Results

This chapter highlights the main results for the project. There were many simulations and many results observed but only the useful ones are presented. The results for the new models were compared with the results of the reference model. The individual results for the reference model are presented in appendix A. If the overall results for a model would match well with the reference then the need of the computational time was investigated. If results do not match, the computational time is not investigated and not presented in this project.

5.1 5-beam method

In this section the results for the 5-beams will be presented. Initially, the optimization was done for each specific specimen. Firstly, the force-displacement was optimized for shear testing and when the curves matched well, the parameters were used for the other two tests as well. The individual optimisation was done for peel and shear as well. Lastly, all three coupon tests were optimized simultaneously to match the curves. The optimisations were only considering the parameters mentioned in 4.2.1.2.

5.1.1 Shear parameter identification

In this test the curves matched well for the shear test, see Figure 5.1. The data is written in Table 5.1. They fail almost at the same force level with 0.6% in difference and an noticeable difference in displacement with 13.0% difference, with the 5-beam failing later.

The data from Table 5.1 were then used as input for both peel test and u-tension simulations. The curves did not match for neither of them, where they fail later than the shear test. The force-displacement curves for peel compared to the reference can be seen in Figure 5.2. The peel test did not fail in the same control time as with the reference, it failed much later which cannot be seen in the figure. However, after 3.8 mm the first beam for the peel fails and the force level drops 17.5%.

Table 5.1: The parameter identification for the shear test.

E	EFAIL	ET	SIGY	Beam distance from mid-point
45.03	0.10	1.70	2.02	1.5 mm

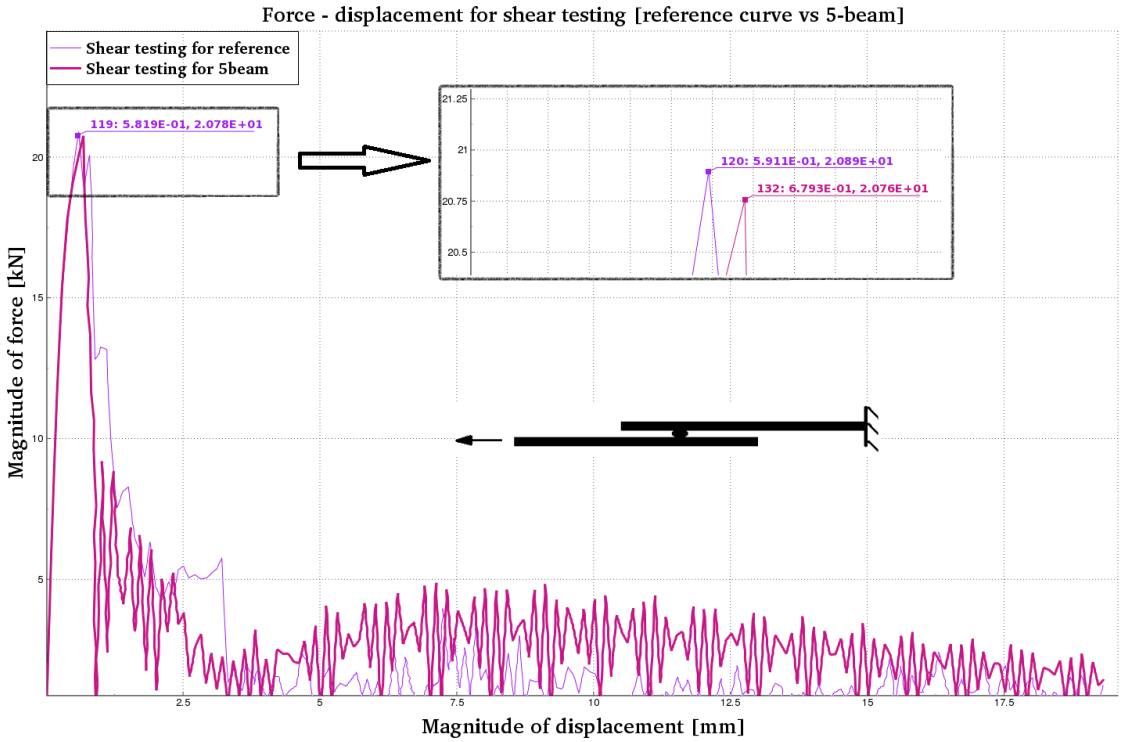

Figure 5.1: Comparison between optimised parameters for lap-shear 5-beam vs the reference lap-shear.

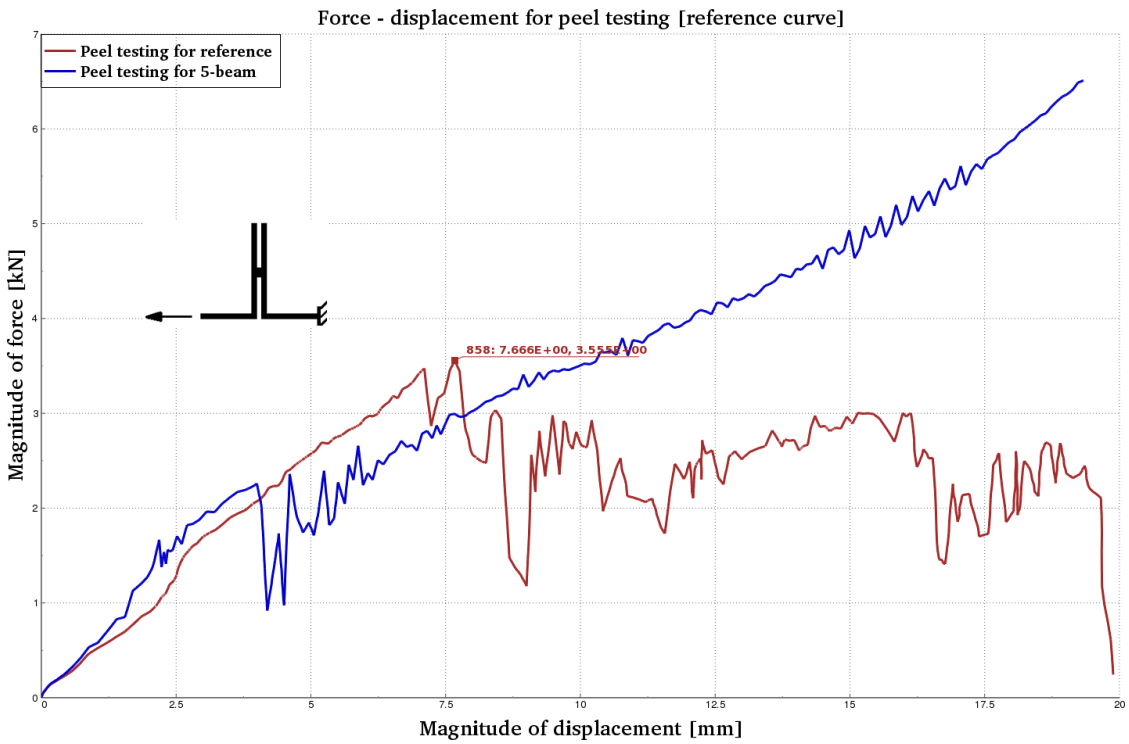

Figure 5.2: Parameters taken from Table 5.1 and used for peel testing.

For the u-tension test, initially the curve for 5-beam matched well with the reference but when the reference fails the 5-beam continues without failing. Again, for the same control time the u-tension did not fail. The difference in force level when the reference fail was 10%.

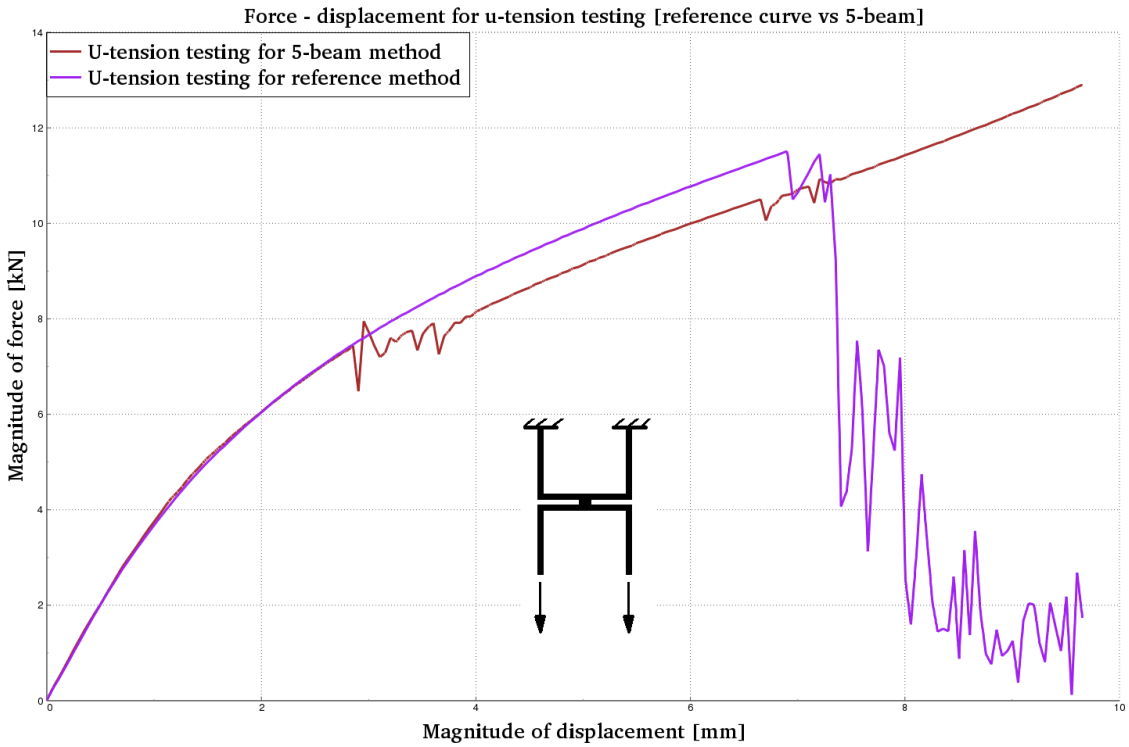

Figure 5.3: Parameters taken from Table 5.1 and used for u-tension testing. The 5-beam does not fail withing the same displacement and force as the reference.

Table 5.2: Percentage difference in force-displacement compared with reference for shear parameter identification

Variants	Δ Force	Δ Displacement
Shear	-0.6%	+13.0%
Peel	No failure	-
U-tension	No failure	-

5.1.1.1 U-tension parameter identification

The u-tension for 5-beam is well matched with the reference thanks to the new optimisation. The displacement of the failure of the beams are almost the same (1% difference), however the force level of the failure differs with 9.0%. Where the 5-beam had the lower level.

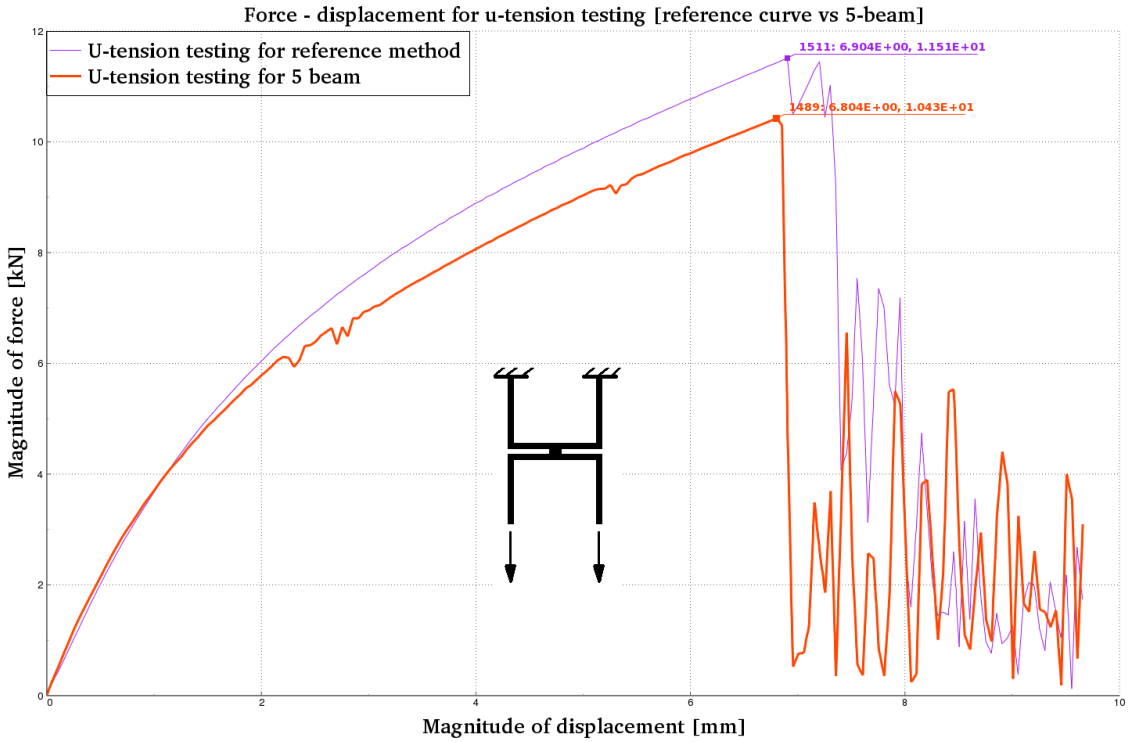

Figure 5.4: Parameters taken from Table 5.3 and used for u-tension testing.

Table 5.3: The parameter identification for the u-tension test. The parameters gives a good matching curve with the reference model.

E	EFAIL	ET	SIGY	Beam distance from mid-point
285.0	0.12	0.5	1.0	1.5 mm

When testing the same data from Table 5.3 for shear and comparing with the reference, the difference is more clear. The force level is 51.0% lower and the displacement is 36.0% earlier.

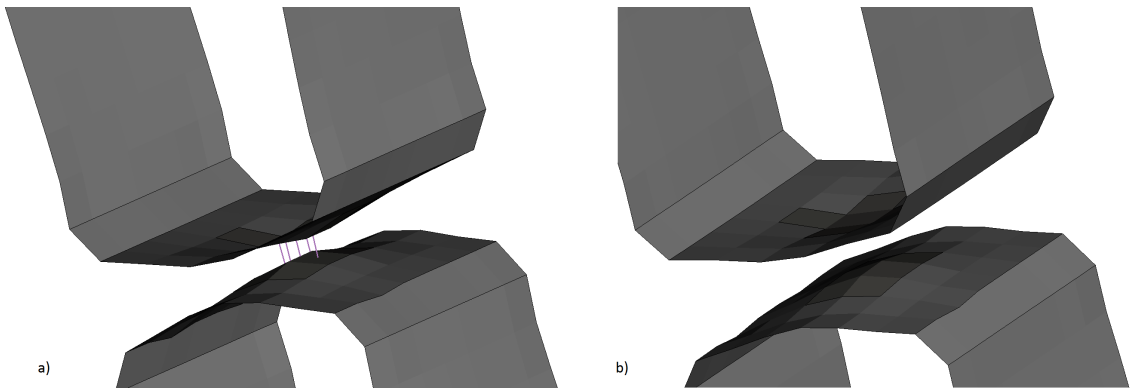

Figure 5.5: The u-tension test a) the beams reach the limit and b) the beams fail without effecting the HAZ.

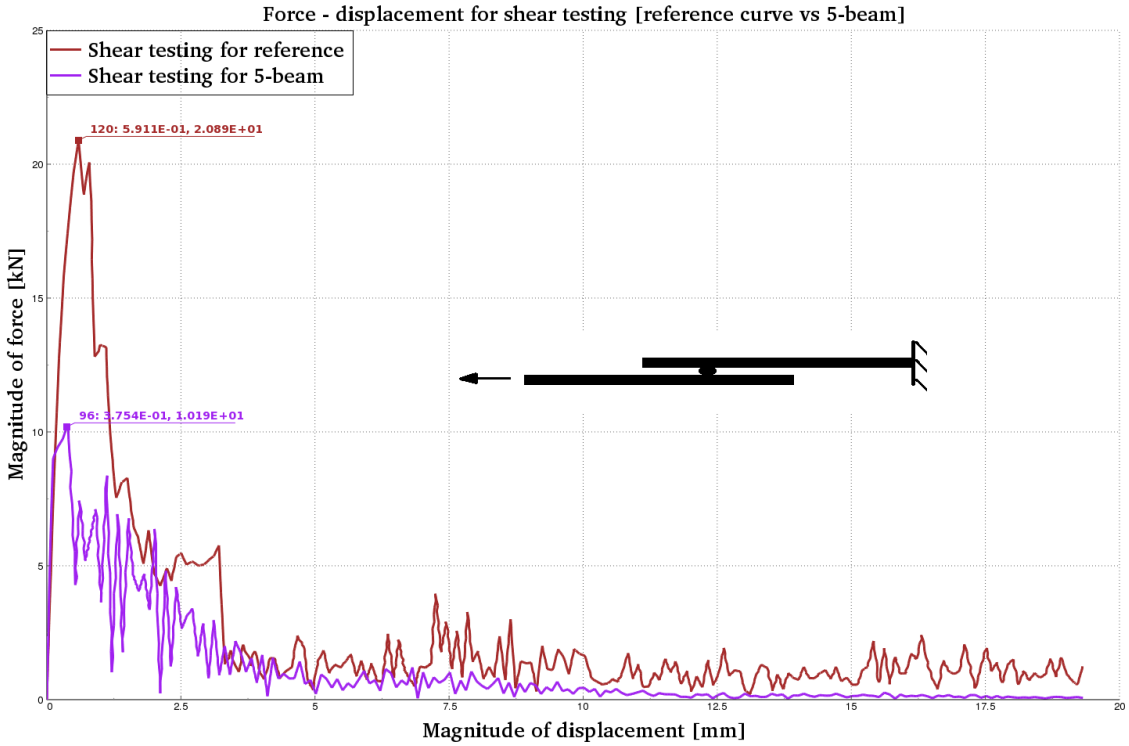

Figure 5.6: Parameters taken from Table 5.3 and used for shear testing.

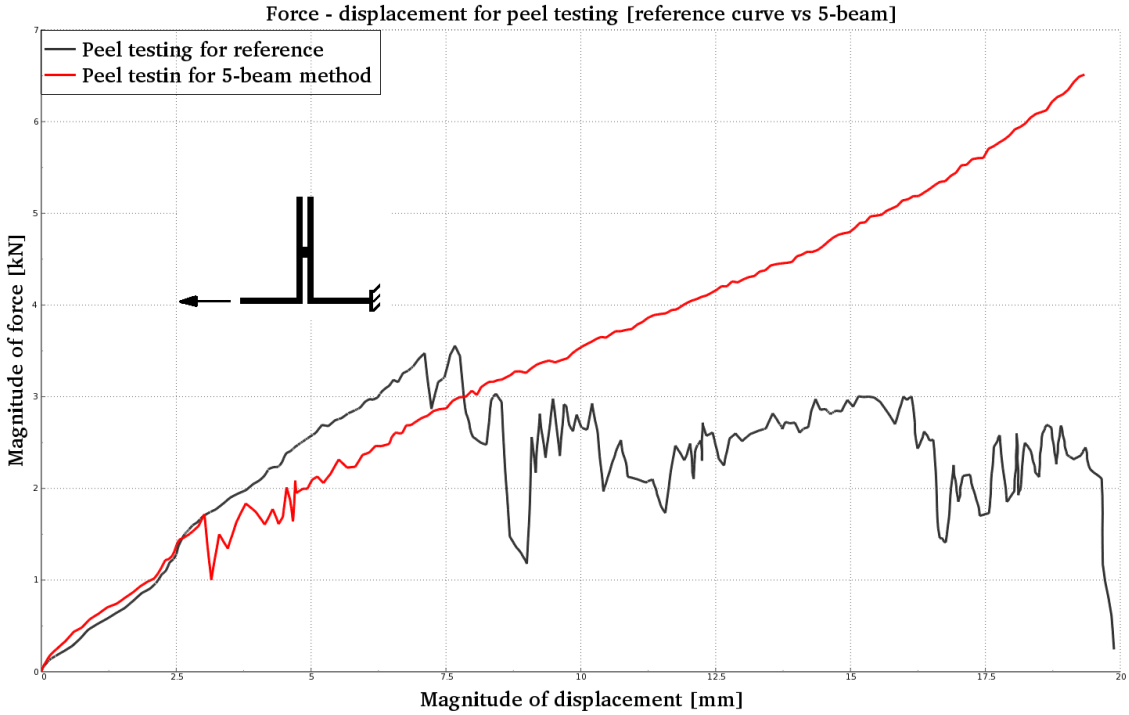

Figure 5.7: Parameters taken from Table 5.3 and used for peel testing.

For the peel test the 5-beam did not fail during the same control time. It failed much later. The first beam failed after 3 mm and the force level dropped with 17.0% but the rest of the beams remained during the control time.

Table 5.4: Percentage difference in force-displacement compared with reference for u-tension parameter identification

Variants	Δ Force	Δ Displacement
U-tension	-9.0%	-1.0%
Shear	-51.0%	-36.0%
Peel	No failure%	-

5.1.1.2 Peel parameter identification

The curves do not match well for the peel optimisation, see Figure 5.8. The peel test differs from the other two coupon tests where the nugget takes up forces in x- and y-direction. Unlike the shear and the u-tension where forces are in one direction.

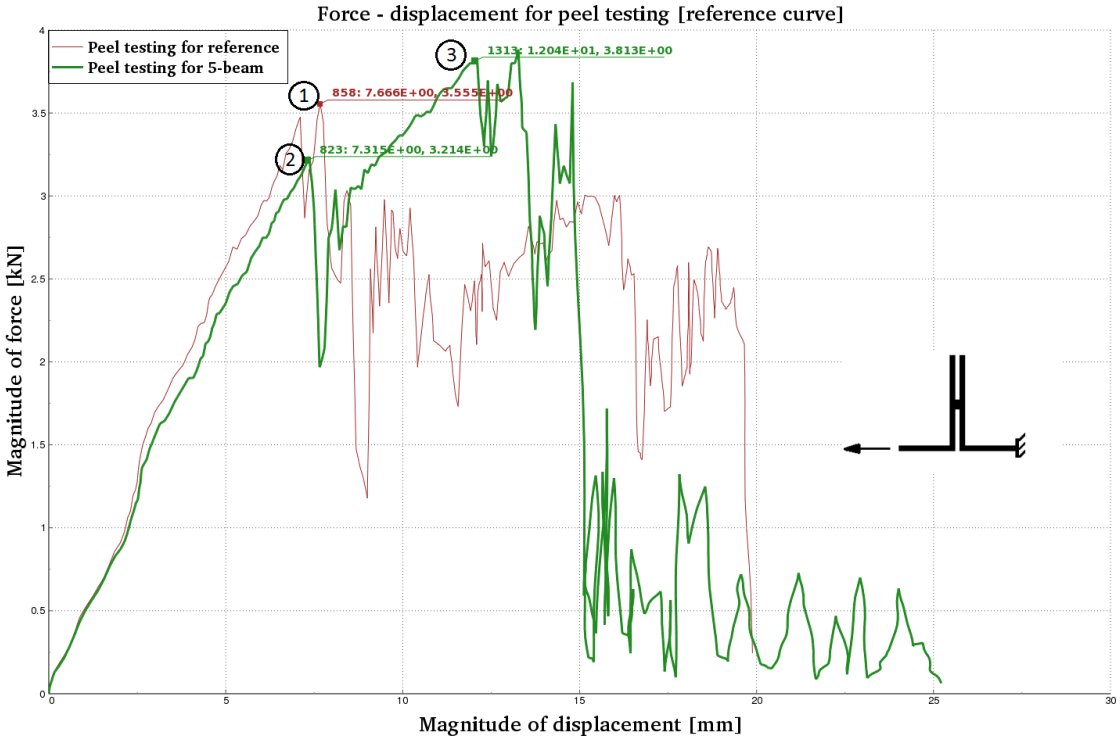

Figure 5.8: Parameters taken from Table 5.5 and used for peel testing. 1) The reference model failed. 2) 1 beam failed for the 5-beam and the force level is dropped. 3) The 5-beam finally fails.

The displacement for the 5-beam when it fails was 57.0% later and the force was 7.0% higher. Before the 5-beam failed completely, 1 beam out of 5 failed at 7.32 mm and 3.2kN. This was very close to the failure of the reference. But the definition of

the failure of the whole spot weld is not fulfilled here, where all the beams have to fail. After the failure of 1 beam, the force level dropped with 11.0% for the 5-beam method.

Table 5.5: The parameter identification for the peel test. The parameters gives an okay matching curve with the reference model.

E	EFAIL	ET	SIGY	Beam distance from mid-point
285.00	0.12	0.5	2.00	1.5 mm

The same parameters from Table 5.5 were used for the u-tension. The matching of the curves in the beginning was well until the reference failed. The reference failed at 6.9 mm and 11.5 kN and the 5-beam failed at 9.1 mm and 12.4 kN. It was 32.0% later in displacement and 7.5% higher in force level.

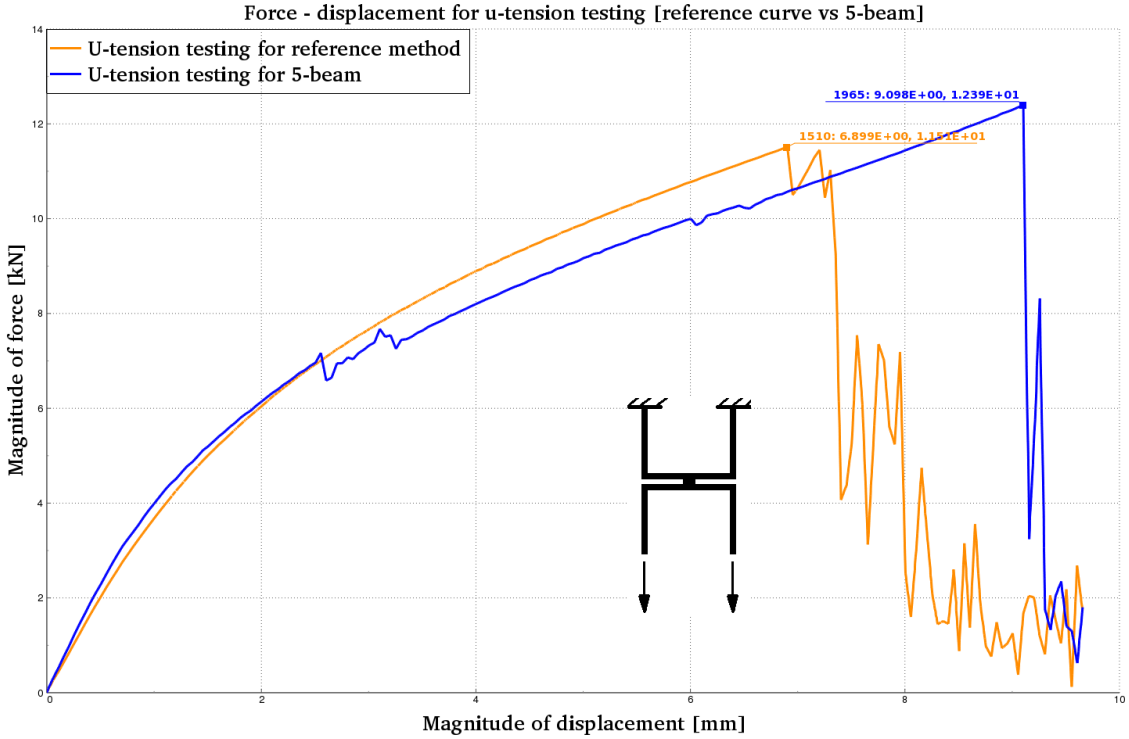

Figure 5.9: Parameters taken from Table 5.5 and used for u-tension testing.

Testing the parameters from Table 5.5 gave better results than for the shear. The displacement was 1.5% less and the force level was 5.5% lower.

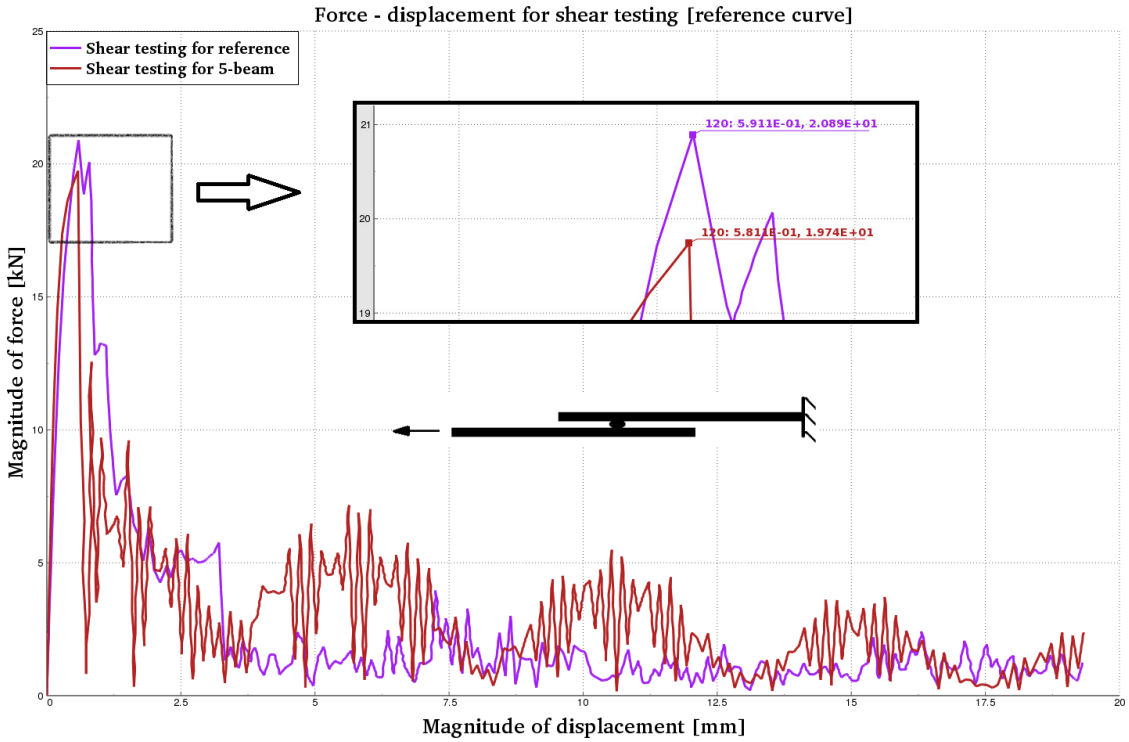

Figure 5.10: Parameters taken from Table 5.5 and used for shear testing.

Table 5.6: Percentage difference in force-displacement compared with reference for peel parameter identification

Variants	Δ Force	Δ Displacement
Peel	+7.0%	+57.0%
U-tension	+7.5.0%	+32.0%
Shear	-5.5%	-1.5%

5.1.2 Final results for 5-beam

The results presented in this section shows simulations where the 3 coupon tests were all set up to be optimised at once to respective reference model. Therefore the optimisation used is taken all 3 configurations into account at once. The results for respective test are shown in Figures 5.11-5.12. In the end of the results of 5-beam, a summarized Table of the results is presented, see Table 5.9.

Table 5.7: The parameter identification for the final simulations.

E	EFAIL	ET	SIGY	Beam distance from mid-point
240.0	0.15	0.9	1.5	1.5 mm

5.1.2.1 Peel testing

The displacement for the peel test for 5-beam is 40.0% higher and the force level is 30.5% higher. The HAZ breaks which means that the spot weld has failed, see Figure 5.12.

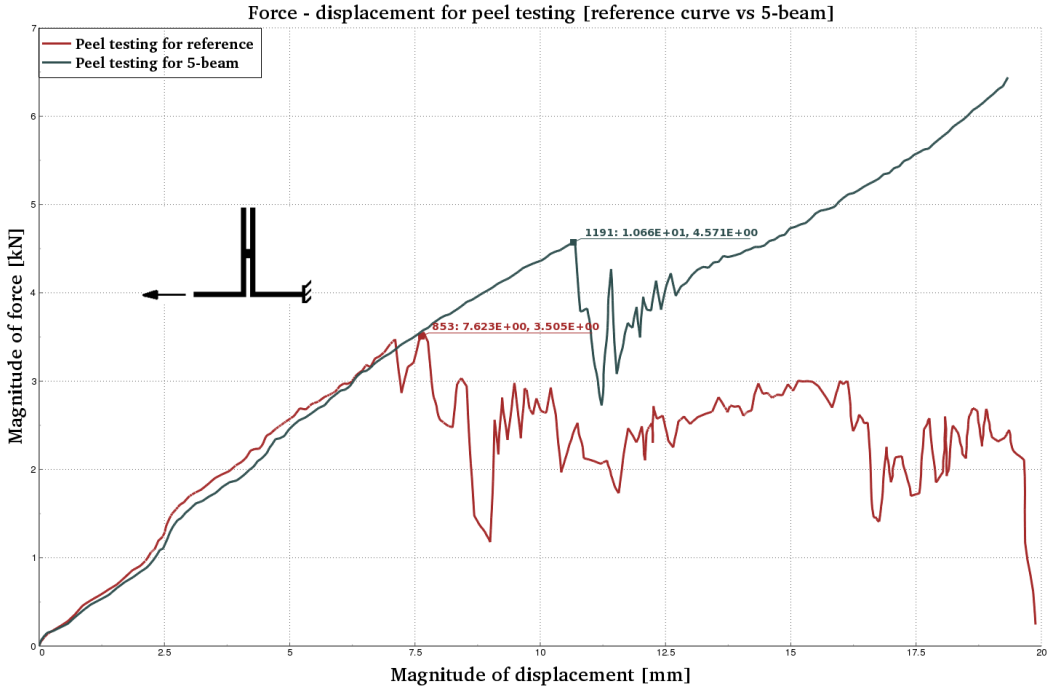

Figure 5.11: The curve for 5-beam does not fail and in comparison with the reference they do not match.

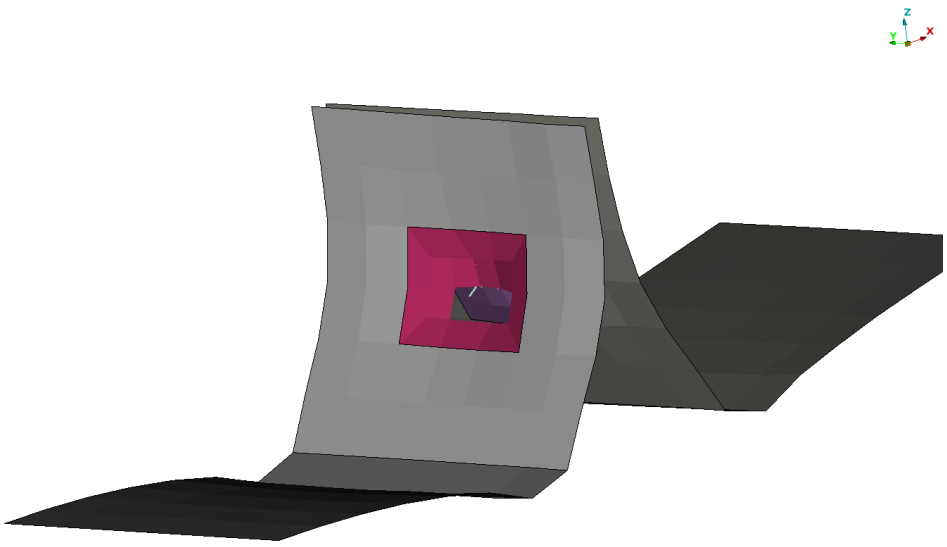

Figure 5.12: Failure of the peel test where the HAZ breaks.

5.1.2.2 U-tension testing

The resulting curve follows the reference curve before the failure for the u-tension. The failure of the reference is earlier and the 5-beam fails with 13.3% higher force level and 37.4% more displacement. Figure 5.13 shows the HAZ failing, where 1 element on the upper sheet has failed.

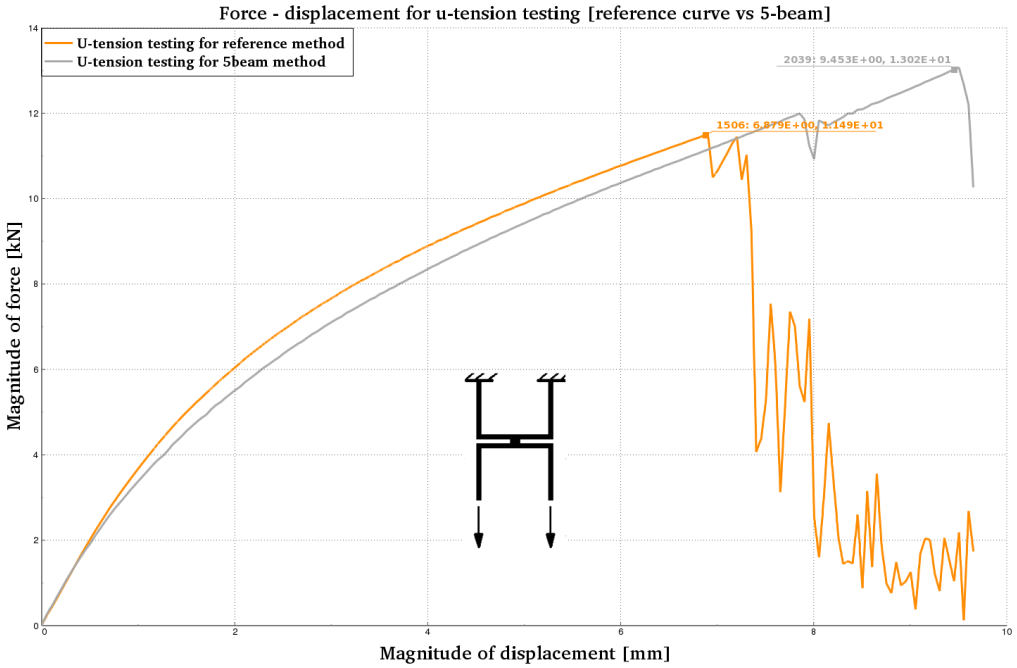

Figure 5.13: Matching curves between reference and 5-beam and the 5-beam fails later.

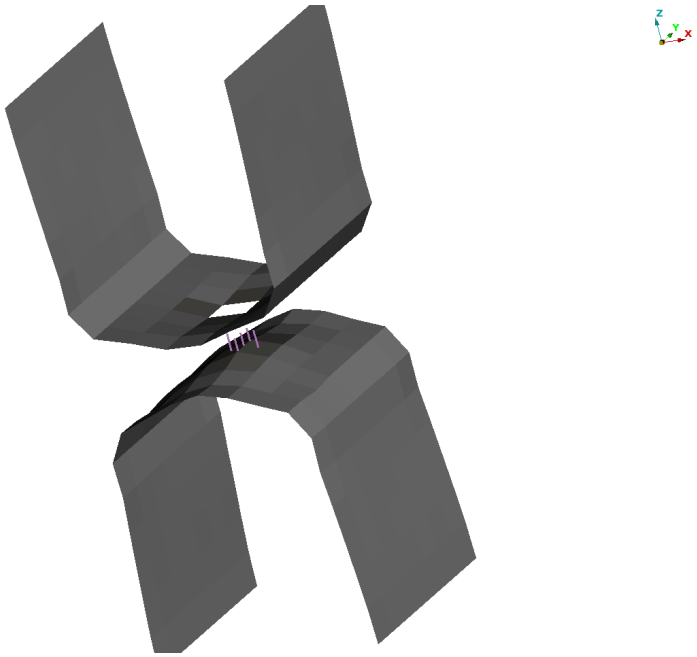

Figure 5.14: Failure of the u-tension test where the HAZ breaks.

5.1.2.3 Shear testing

The curves do not follow the same path and it can be seen in Figure 5.15. The failure occurs 200% later in the displacement comparison and 30.1% higher force level.

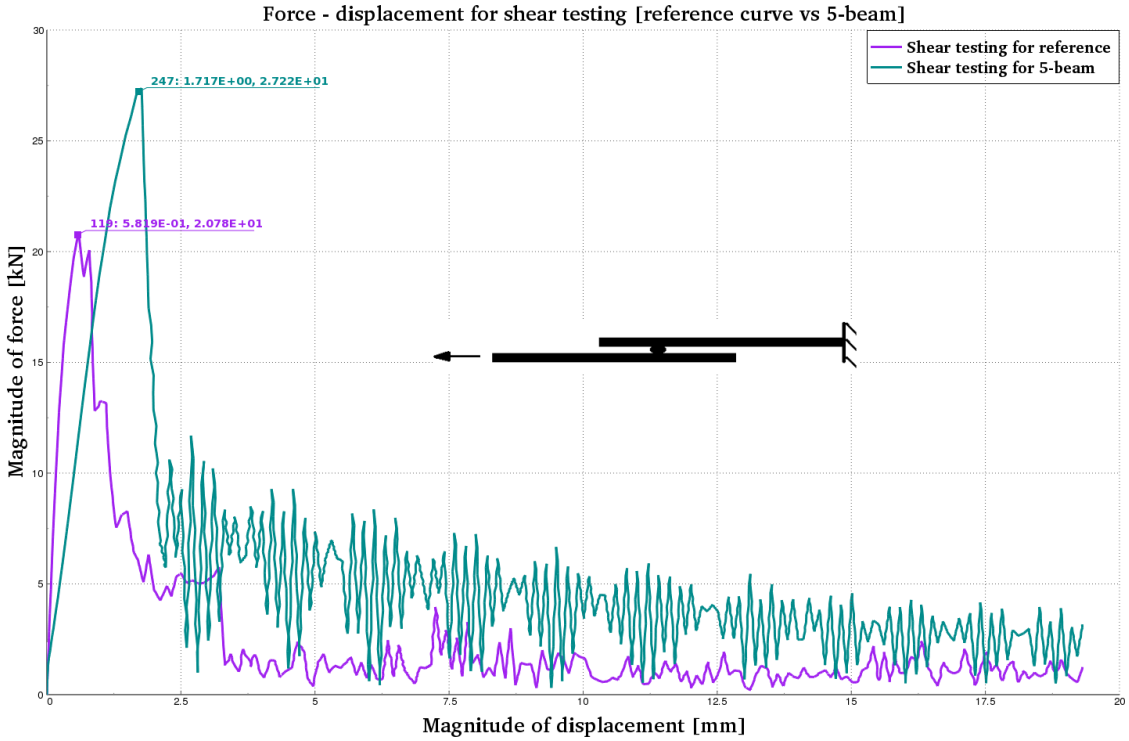

Figure 5.15: The reference curve vs the 5-beam final results for shear.

The 5-beam shear test fails later and with more force, see Figure 5.15

Table 5.8: Percentage difference in force-displacement compared with reference for final results of the parameter identification

Variants	Δ Force	Δ Displacement
Peel	+30.5%	+40.0%
U-tension	+13.3%	+37.4%
Shear	+30.1%	+200.0%

Table 5.9: Summarized results for 5-beam optimisation.

Setup of 5-Beam optimisation for:	**Shear**	**U-tension**	**Peel**
Shear identification	OK	Bad	Bad
U-tension identification	Bad	Good	Bad
Peel identification	Good	Bad	Bad
Final results	Bad	Bad	Bad

5.2 8-beam and 9-Beam method

U-tension specimen were simulated with all the variants of 8-beam and 9-beam methods. The resulting curves for u-tension are shown in Figures 5.16, 5.17, 5.18. The Figure 5.16 shows stiffness curves comparison between reference model and 9-beam method. From the figures, it is quite clear that 9-beam method is not an viable replacement for reference method. This can be attributed to huge difference in force levels (about 15%) and displacement levels at failure (about 35%) for either values of Young's modulus.

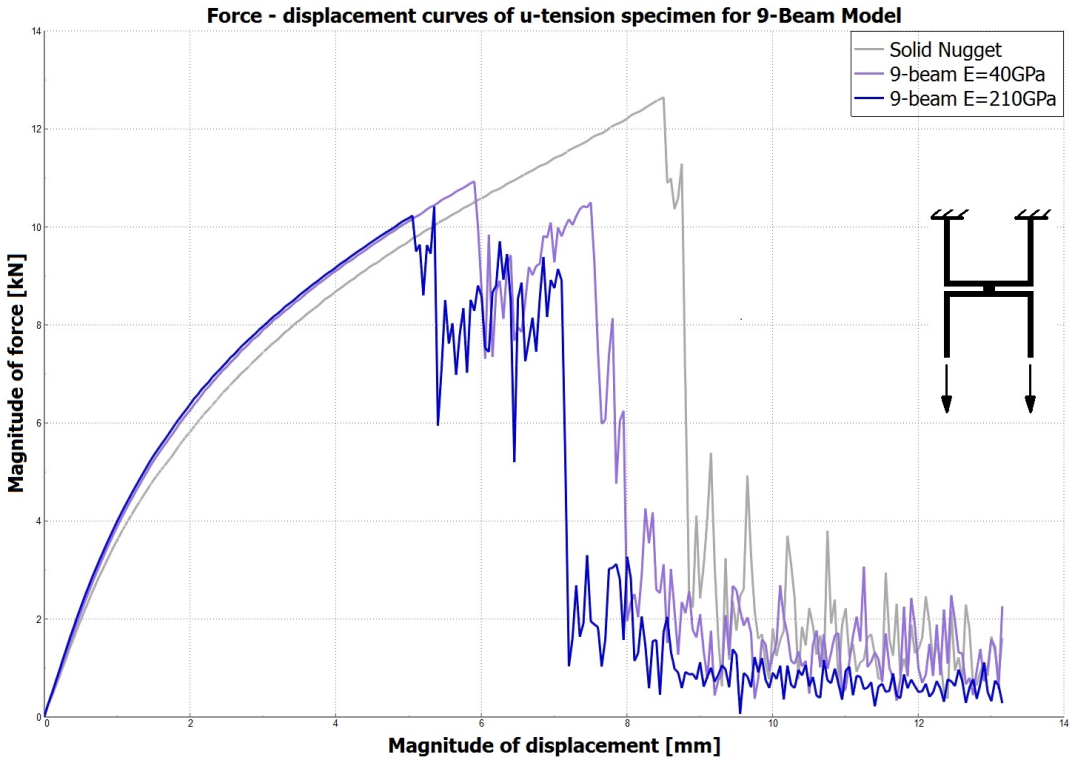

Figure 5.16: Comparison of stiffness curves for u-tension specimen between reference model with solid nugget and 9-beam model

From the Figure 5.17, it is visible that when shell elements of base material exist in the centre of beams, the stiffness curves are not matching the reference curves. The difference is substantial for both force levels (about 17%) and displacement levels (37%) at failure. Thus, the 8-beam without a cavity is not a viable replacement for reference method.

When 8-beams method with cavity in the region between beams is used, the stiffness curves represent the reference model stiffness curves better than other variants. Of the two variants within the same model, the model using Young's modulus of 40GPa on the beams match the reference stiffness curve more closely.

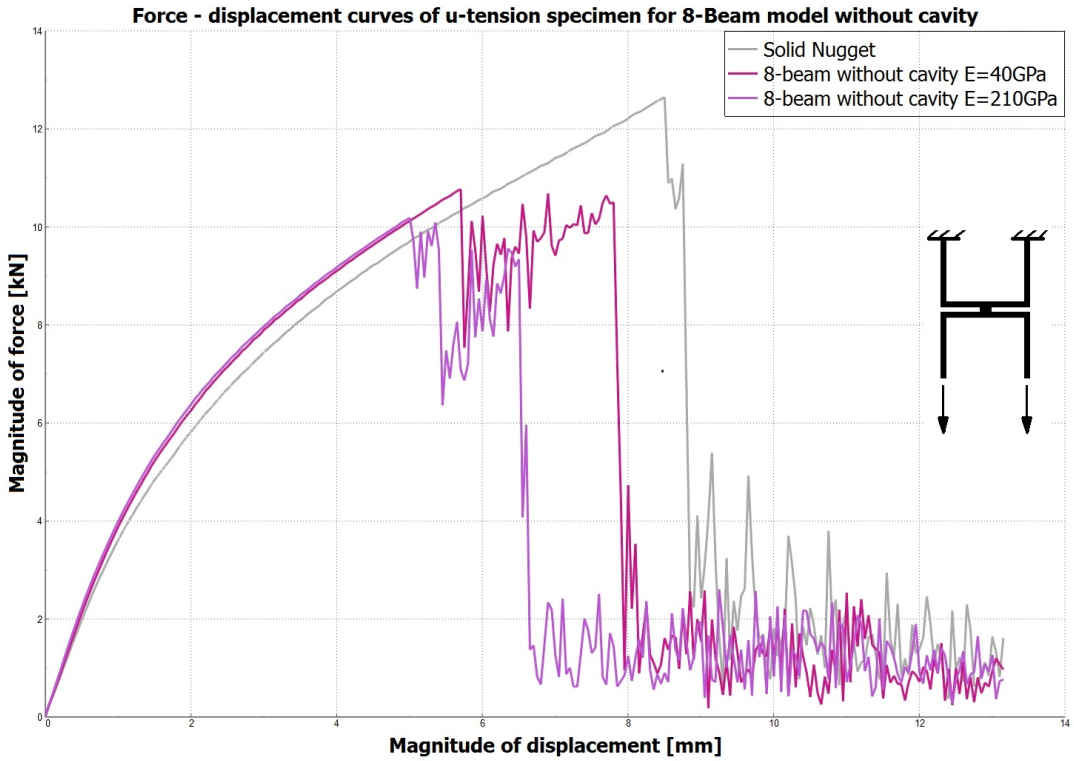

Figure 5.17: Comparison of stiffness curves for u-tension specimen between reference model and 8-beam model without cavity in the region between beams

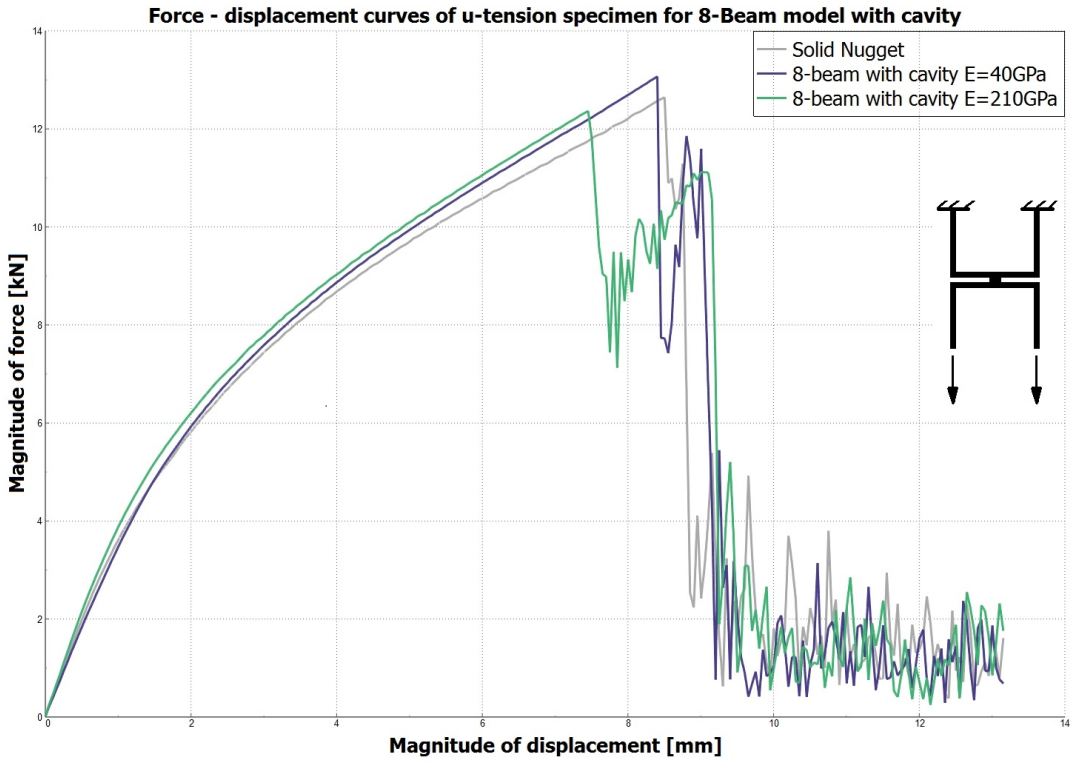

Figure 5.18: Comparison of stiffness curves for u-tension specimen between reference model and 8-beam model with cavity in the region between beams

Table 5.10: Percentage difference in force-displacement levels for u-tension specimen between reference and 8-beam model with a central cavity

Variants	Difference in force	Difference in displacement
Young's Modulus = 40 GPa	3.35%	1.18%
Young's Modulus = 210 GPa	2.20%	12.35%

From the above result, it is noted that 8-beam model with central cavity between beams could be viable replacement for reference model. To confirm this, the 8-beam model with cavity must be tested with other coupon test (peel an lap shear) as well.

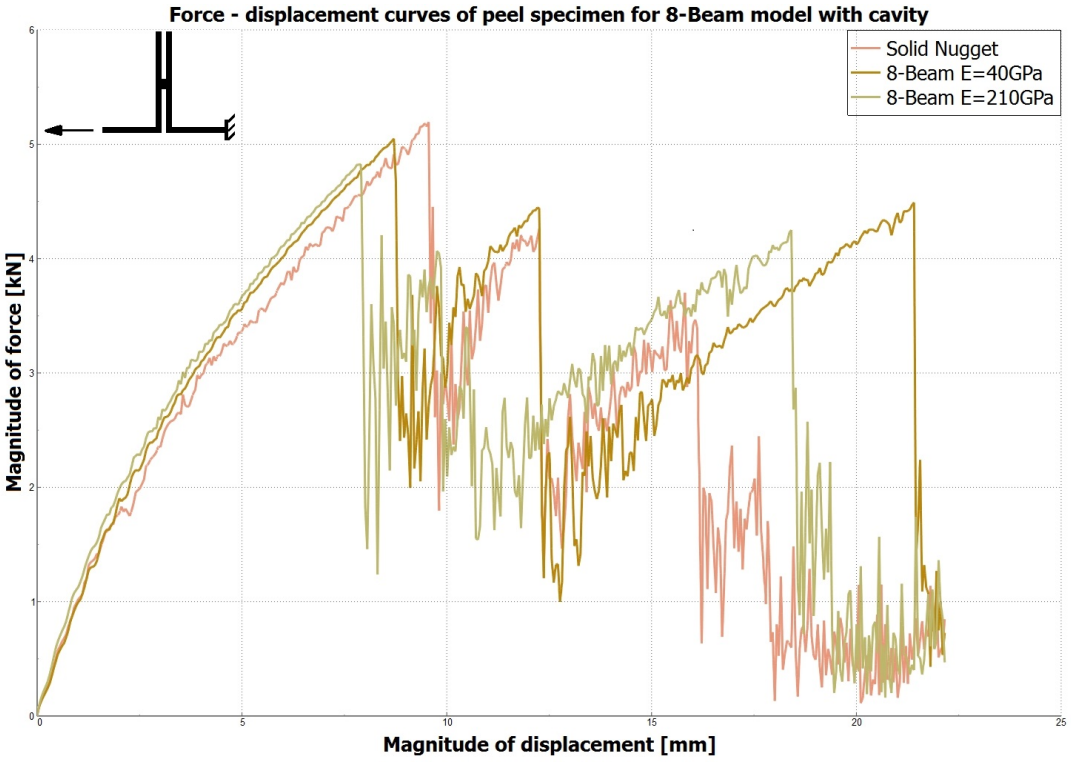

Figure 5.19: Comparison of stiffness curves for peel specimen between reference model and 8-beam model with cavity in the region between beams

When 8-beam model with cavity is tested with peel test, the stiffness curves as shown in Figure 5.19. From the stiffness curve, it is observed that the 8-beam model with Young's modulus of 40 GPa is closely representing reference curves. The Table 5.11 shows the difference in terms of percentage.

Table 5.11: Percentage difference in force-displacement for peel specimen levels between reference and 8-beam model with a central cavity.

Variants	Difference in force	Difference in displacement
Young's Modulus = 40 GPa	2.78%	8.88%
Young's Modulus = 210 GPa	7.02%	17.25%

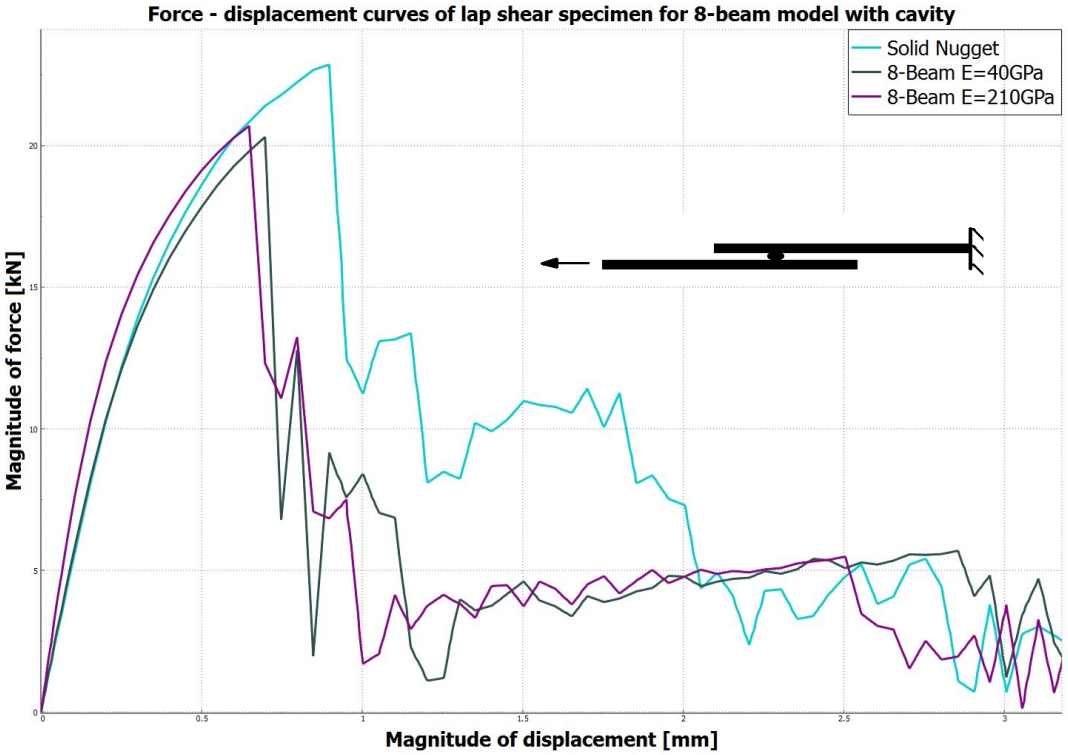

Figure 5.20: Comparison of stiffness curves for lap shear specimen between reference model and 8-beam model with cavity in the region between beams.

The stiffness curves for lap shear specimen simulation with 8-beam with cavity variants are shown in Figure 5.20. The percentage difference is mentioned in the Table 5.12. There exists a substantial difference in magnitude of displacement at failure.

Table 5.12: Percentage difference in force-displacement for lap shear specimen levels between reference and 8-beam model with a central cavity

Variants	Difference in force	Difference in displacement
Young's Modulus = 40 GPa	11.17%	22.28%
Young's Modulus = 210 GPa	9.48%	27.83%

From the above stiffness curves, notable failure variants are 9-beam and 8-beam without cavity. The 8-beam model with cavity exhibit a good correlation with reference curve when failure mode does not involve shear. The good correlation with u-tension, peel specimen and poor correlation with lap shear specimen come as evidence for the same.

Table 5.13: Simulation time in seconds for various models.

Specimen	Model	Simulation Time (seconds)
U-tension	Reference	36
	E = 40GPa	39
	E = 210GPa	38
Peel	Reference	51
	E = 40GPa	51
	E = 210GPa	52
Lap shear	Reference	27
	E = 40GPa	27
	E = 210GPa	25

From Table 5.13, it can be noted that irrespective of modes of failure, the simulation time remains within cushion of variation. The time cushion observed through various simulation is up to 2 seconds, due to variation in performance of different cores.

5.3 GISSMO Method

5.3.1 GISSMO material cards from previous study [1]

The GISSMO cards from earlier project [1] were simulated for compatibility with HAZ and results are shown in Figures 5.21, 5.22, and 5.23.

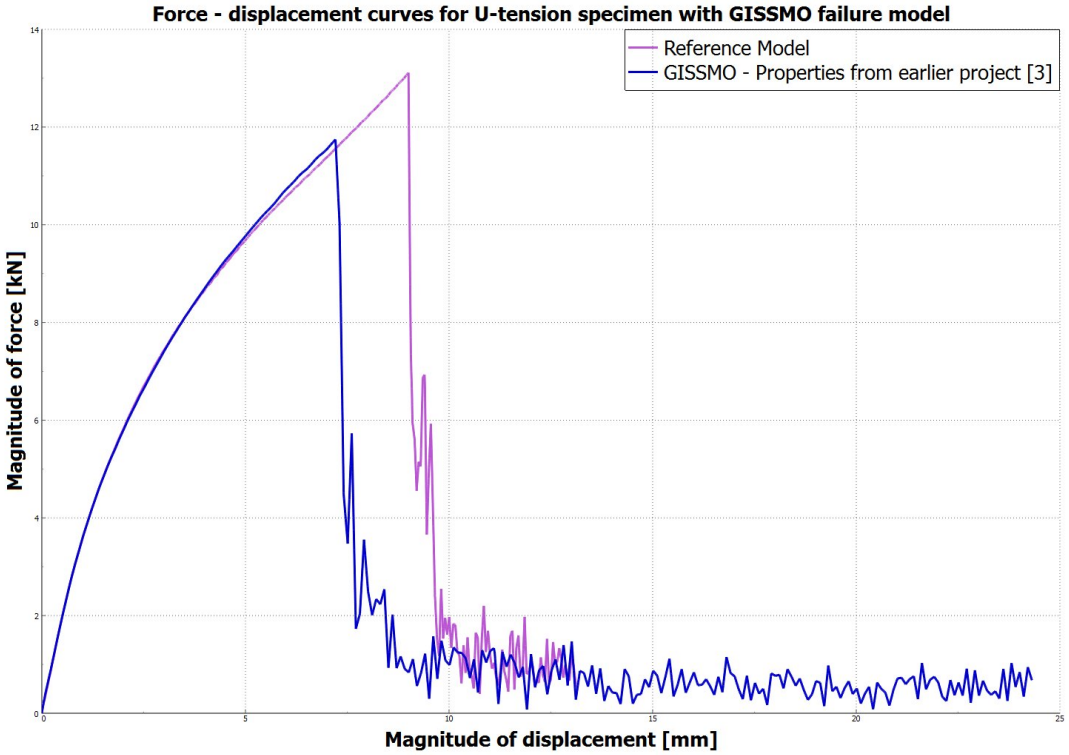

Figure 5.21: Comparison of stiffness curves for u-tension specimen between reference CrachFEM failure model with GISSMO failure model.

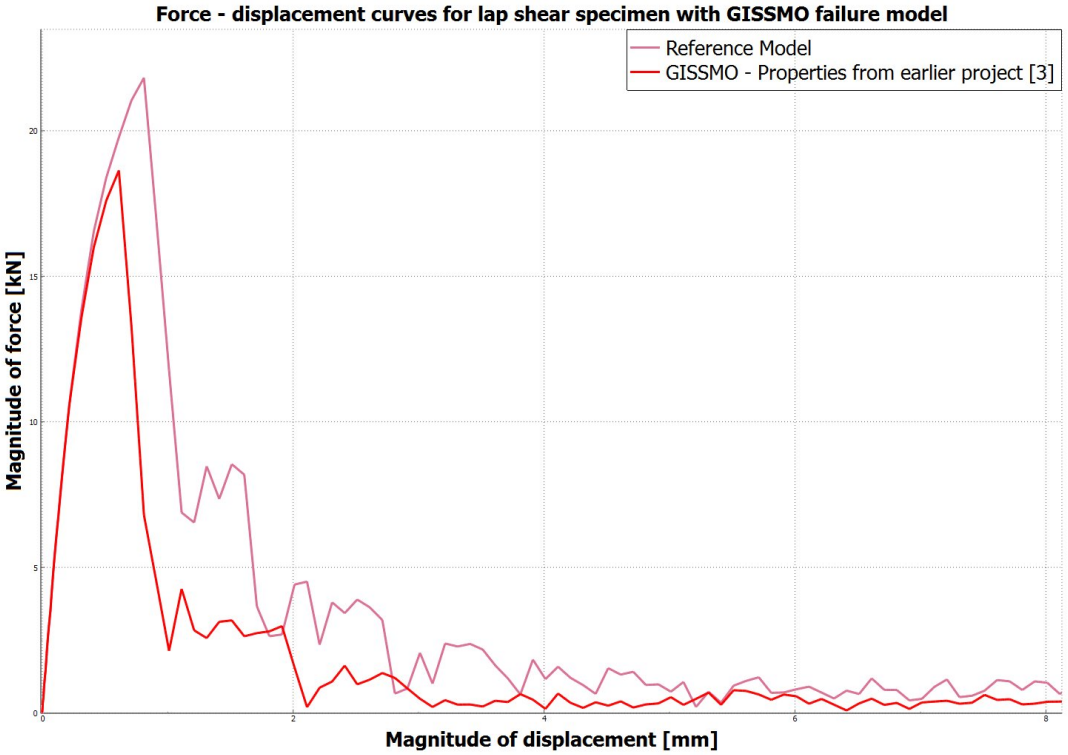

Figure 5.22: Comparison of stiffness curves for lap shear specimen between reference CrachFEM failure model with GISSMO failure model.

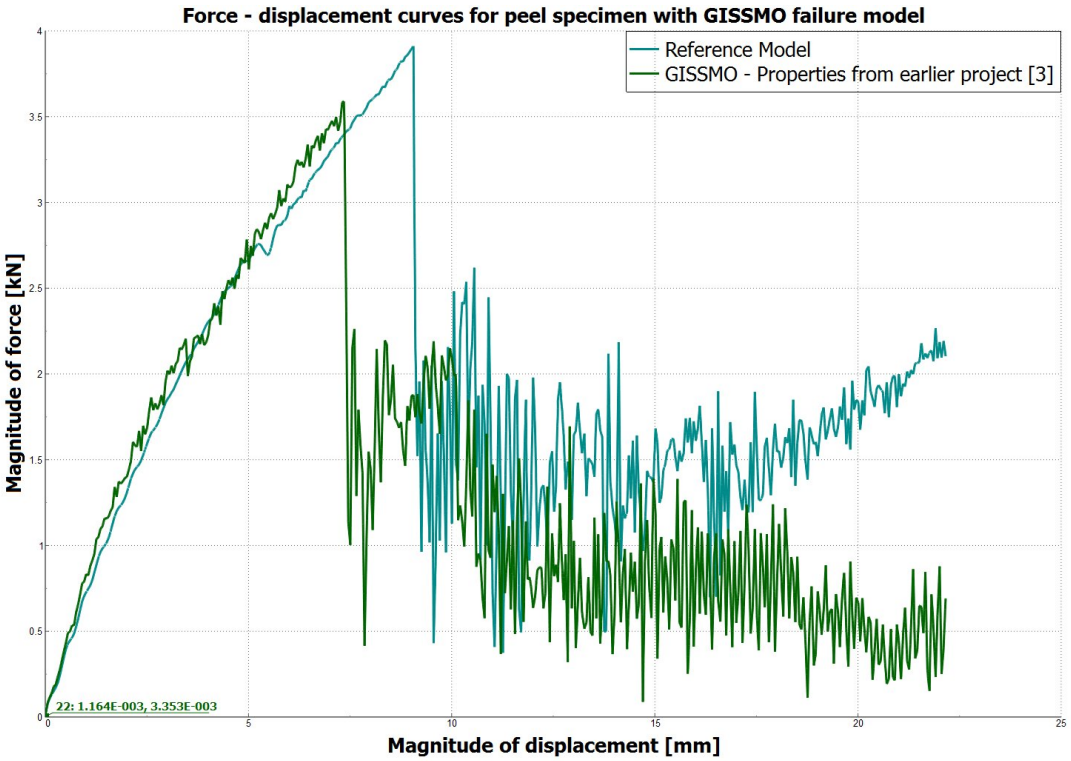

Figure 5.23: Comparison of stiffness curves for peel specimen between reference CrachFEM failure model with GISSMO failure model.

From the above results, it is observed that stiffness curves of GISSMO material cards developed by previous project do not match the stiffness curves of reference model with CrachFEM failure. This variation was attributed to mesh dependency and other properties (Element Form - ELFORM and Hourglass ID - HGID). With appropriate settings, the resulting curve with GISSMO failure model failed to match the reference curves.

5.3.2 Optimisation of GISSMO with coupon test

The difference between the curves was corrected by optimisation of the GISSMO material properties with reference model's stiffness curves. The curve defining stress against strain is retained as before, with optimisation done in the part of triaxiality curves (LCSDG and ECRIT). The tensile side of triaxiality curves are discretized into six stages. The triaxiality curves were optimised with only u-tension coupon test initially. The optimisation was done with u-tension for two reasons:

- To save time taken for optimisation.
- To validate that modification of triaxiality curve will match the reference curve.

After optimising the GISSMO material card with u-tension, the GISSMO material is optimised for all specimens. The results of each coupon test are shown below.

5.3.3 Coupon tests

The stiffness curves of three coupon test with GISSMO material models and reference model are represented in the following picture. Three variations of GISSMO material cards are presented below:

- GISSMO material card properties defined in the project [1]
- Within GISSMO material card, triaxiality parameters are optimised with u-tension specimen
- Within GISSMO material card, triaxiality parameters are optimised with three coupon tests

The behaviour of stiffness curves with GISSMO failure model closely represent CrachFEM failure model. The displacement at which failure happens was controlled by changing ECRIT and LCSDG curves.

In the Figure 5.24, representing stiffness curves for reference model with CrachFEM failure model and developed GISSMO failure model, it can be observed that the GISSMO model's stiffness curves follows the path of CrachFEM model, except the fact that failure occurs at different instances. For GISSMO card from earlier project, the failure occurs much sooner. With optimised GISSMO material cards, the failure occurs much closer to reference model. The percentage difference are represented in Table 5.14.

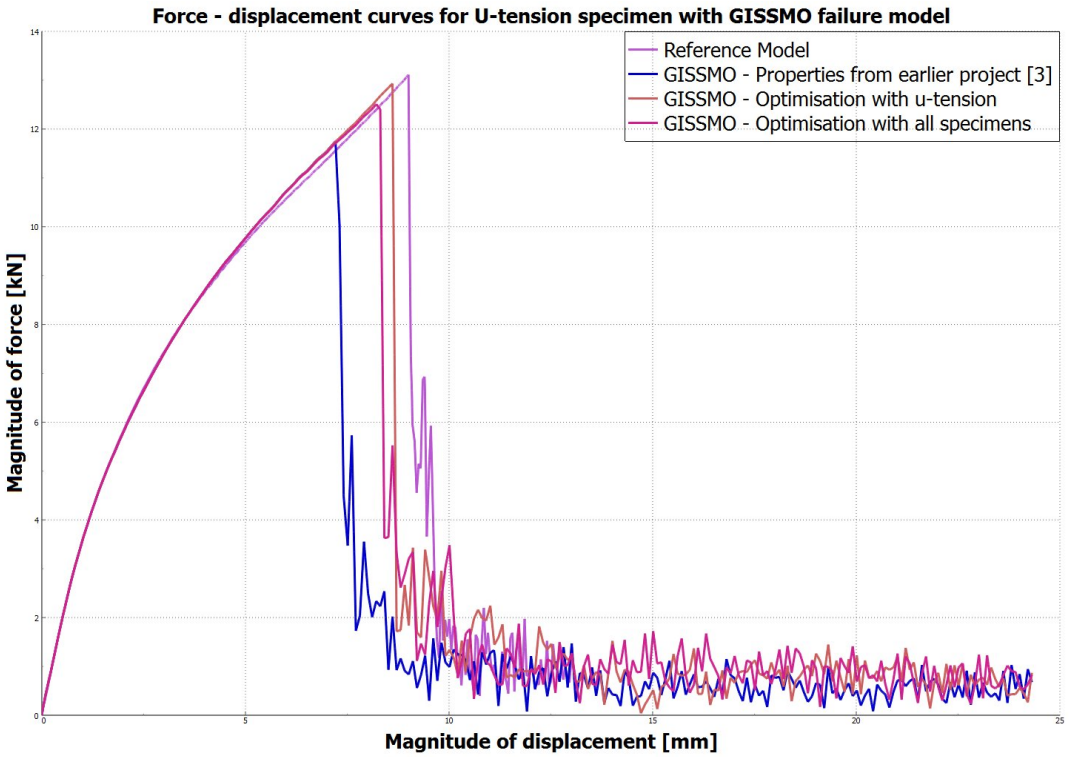

Figure 5.24: Comparison of stiffness curves for u-tension specimen between reference CrachFEM failure model with GISSMO failure models

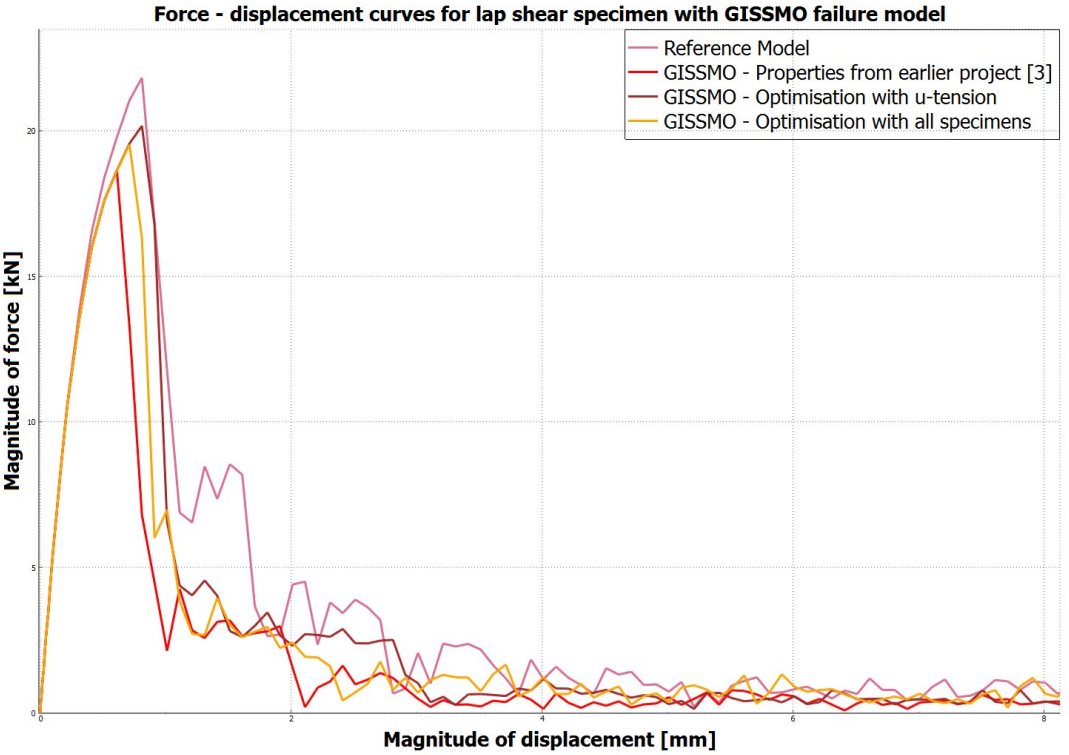

Figure 5.25: Comparison of stiffness curves for lap shear specimen between reference CrachFEM failure model with GISSMO failure models

For lap shear specimen, the stiffness curves for GISSMO failure follows the reference curve, until a force level of 15kN. Beyond that, GISSMO behaviour deviates from original curve irrespective of optimisation the triaxiality curves. This is attributed to *MAT_024 part of material card, which defines the hardening curve. The displacement level at failure is matched to the reference curve by optimisation with coupon test. It is seen from the Figure 5.25 that GISSMO, when optimised with all specimens, is better than GISSMO material card from earlier project. But, it falls short of CrachFEM reference curve. Interestingly, when optimised with u-tension alone, the curve matches the reference curve better.

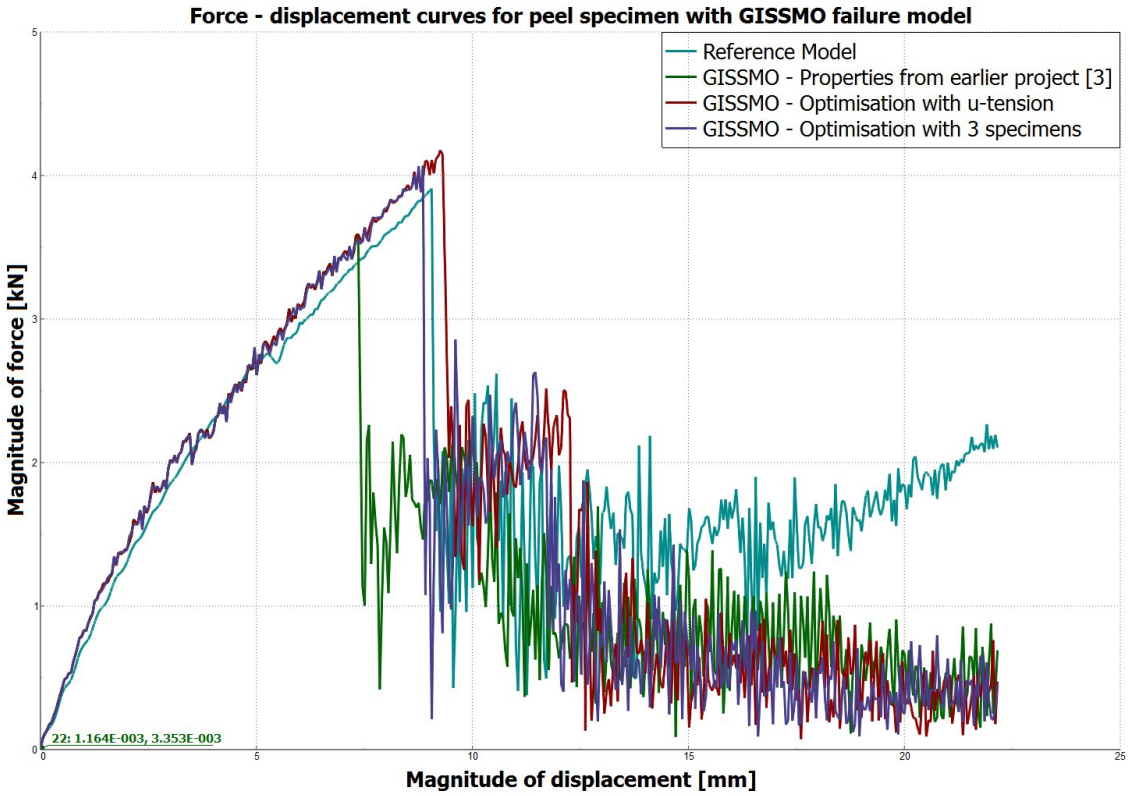

Figure 5.26: Comparison of stiffness curves for peel specimen between reference CrachFEM failure model with GISSMO failure models

For peel test specimen, the GISSMO material card from earlier project seem to follow the reference curve perfectly but falls short in displacement at failure. The GISSMO material model after optimisation with u-tension, overshoots the reference curve in both force levels and displacement. The GISSMO material card, when optimised for all coupon test, represents the CrachFEM curve closely. The force levels are on higher side and the displacement on lower side. The difference in force and displacement levels are represented in Table 5.14.

Table 5.14: Percentage difference in levels of force and displacement at the instant of failure

	U-tension specimen		**Lap shear specimen**		**Peel specimen**	
	ΔF	**Δd**	**ΔF**	**Δd**	**ΔF**	**Δd**
GISSMO (From project [3])	10.43	19.92	14.58	24.61	8.18	18.82
GISSMO (Triaxiality parameters optimised for u-tension)	1.39	4.35	7.57	0	6.75	2.18
GISSMO (Triaxiality parameters optimised with three coupon tests)	4.61	8.81	10.52	12.27	4.02	2.26
* ΔF = Difference in force & Δ d = Difference in displacement						

5.3.4 Simulation time

The three specimens were modelled into same file and run with variants of GISSMO failure model and reference CrachFEM failure model. The simulation time is shown in Table 5.15.

Table 5.15: Simulation time for the CrachFEM and GISSMO failure model

Modelling	**Simulation Time (seconds)**
Reference (CrachFEM)	45
GISSMO (From project [3])	28
GISSMO (After initial optimisation with u-tension specimen only)	27
GISSMO (After optimisation with three coupon test specimens)	28

It can be noted that the simulation time is affected hugely by failure model. CrachFEM takes around 37% more time to simulate failure of a spot weld compared to the GISSMO failure model. This is due to reason that CrachFEM being an encrypted material model. LS-DYNA is coupled to this black box through a user material interface. As LS-DYNA has to reach a separate entity outside its environment, it

takes significant amount of time. The GISSMO failure model is represented within the material card, making access to the data easier.

Table 5.16: Summarized table for the final results of the project.

Optimisation for method:	**Shear**	**U-tension**	**Peel**
5-Beam	Bad	Bad	Bad
8-Beam w/ cavity	OK	Good	Good
8-Beam w/o cavity	Bad	Bad	Bad
9-Beam	Bad	Bad	Bad
GISSMO	Good	Good	Good

6
Discussion

There exist many possibilities to approach the problems of reducing computation time. Alternative modelling the spot weld is one possibility to decrease the time taken for simulations. Of the two alternative methods looked upon in this thesis, interesting discussions derived from observations of results are presented below.

6.1 Beams for modelling spot welds

As observed from the results, the new method of 5-beam spot weld modelling does not match well with the reference model. Changing the mesh around the spot weld and having beams instead of solid elements would decrease the computational time significantly. The change from the reference mesh around the HAZ to the meshing of the 5-beam was that the small shell elements around the HAZ was removed to more coarse mesh. This was to have less computational time due to the smallest elements in the geometry. Nevertheless, the results for the 5-beams modelling was not promising, therefore there was no investigation in how the 5-beam method effected the simulation time.

The change of mesh around the HAZ area, which is the critical area, the elements around the nugget were too coarse and could not provide the same precision as the reference. Then the beams can fail to represent a failure which was one of the criteria of spot weld failure. The individual optimisations were matching well, except for the peel test. But once the parameters were used for the other two coupon tests, the curves did not match as good. This is due to the forces created on the beams. The peel specimen was the one specimen which was the most difficult to satisfy with the reference. Therefore, there is need of more investigation and further simulations to satisfy the criteria.

The results for the change of mesh and nugget from solid to beams did not end up with promising results. However, the change of nugget to 8-beams had very promising results where the force - displacement curves almost matched the reference model for the coupon tests but the time to run the simulations were the same. Yet, usage of beams did have positive effects. Unlike, solid elements for the spot weld, beams do not add mass to the model. Since the beams do not add mass in the simulation, there is no added mass to the model. This is more important in the bigger model where there could hundreds or thousands of added grams of mass to

the model. This does not represent the reality of the simulation and there it might have negative affects on the simulation. To avoid mass scaling the 8-beams can be used instead of the solid nugget, with the exact same mesh.

The reason for the 8-beam and the 9-beam setup was because the reference model has 8 nodes in the interface between solid nugget and HAZ. The tests were ran to investigate if same results could be obtained with the beams as with the reference (solid nugget). Since the beams do not need mass scaling as with the solid elements then the problem with mass scaling would decrease massively. Usage of beams will reduce pre-processing time as beams are used with other CAE software to represent spot weld.

6.2 GISSMO Model

The GISSMO material model produced interesting results with difference levels of variations. A first observation is that the GISSMO material card from the other thesis project cannot be implemented directly with spot weld, as it proved to be less compatible for various coupon tests.

The results after optimisation of GISSMO card's triaxiality curves with coupon tests were optimal triaxiality parameters, which gave results similar to the reference model. The model was tested with two different levels, one being optimisation with only u-tension coupon test and other being optimisation with three coupon configurations. When optimised with u-tension alone, the stiffness curve follows the reference curves closely for two coupon configurations but overshoots slightly for the peel configuration. When the GISSMO material card is optimised with three coupon tests, the stiffness curves for u-tension and lap shear closely represents reference curves, but there is a slightly bigger difference than when optimised with u-tension. For peel specimen, the optimisation with three coupon test resulted in better curves closely representing the reference curves.

The simulation time is largely influenced with the use of the GISSMO model. Being not an encrypted material card format, access is easier for LS-DYNA and thus saving about 37% computation time. A body in white (BiW) contains approximately 5000 spot welds. Saving 37% per spot weld, will save approximately 8 hours on a model that runs for 24 hours with MF GenYld + CrachFEM damage model.

Since the results of the 5-beam method were not promising, a merged version of the methods GISSMO and 5-beams was not carried out.

7
Conclusion

The modeling of a spot weld requires more time than that available for this project. The conclusion for the 5-beam is that the matching of the curves can be done individually and the results for shear and u-tension are more promising than the peel test. But this does not satisfy the requirements for modeling a spot weld. There are far too many parameters than the ones used in this project, therefore there is not enough information to determine whether the beams method will ever work or not. Perhaps there is a method with the 5-beams where the results match much better and it can be used. Therefore even further tests are needed before actually removing the 5-beams as an option.

Using the same setup for the coupon test as the reference model with the 8 beam gives almost the same results as the reference model and it has the same computational time. This indicates the beam solution is not faster to simulate than the solid nugget and the time consumption issue comes from the mesh. However, the mass scaling effect on the nugget issue is solved where the beams do not have added mass. In order to avoid mass scaling and to get results which are closer to reality one can use the 8 beams to simulate crash tests.

Though the GISSMO model does not match the reference curves exactly, the GISSMO material model gives good correlation with reference curves. The huge saving in computation time comes in support of using the model despite slight differences, especially in the initial stage of simulation.

7.1 Future work

What is actually time consuming, for the finite element solver, are the smallest elements in the geometry in the HAZ. If the smallest elements can be bigger and fewer, perhaps a faster simulation can be obtained. Therefore, it is important to put more focus on the mesh around in the HAZ. The test performed in this project was mostly for a mesh of 3.5mm, perhaps the 5-beam method works better with 2.5 mm (or another mesh size) and would not take as much time.

The most critical area is the HAZ, because the reference model does not fail in the nugget but only the HAZ fails. In this project there were simulations with failure both in the nugget and in the HAZ. The results indicate that the HAZ area need more research to obtain the actual properties of it and to handle the simulation of

the HAZ more accordingly to the reality.

The variation in beam distance from mid beam to outer beams was restricted due to two factors. Firstly, the outer beams cannot be too far away from the mid beam because that would make the HAZ region far bigger than it actually is. In a bigger model, the neighbour spot welds would have the same size of the HAZ which would create too much HAZ area in the model and that is not realistic. On the other hand, should the outer beam be closer to the mid, the 4.5mm spot weld would no longer be representative in the same way also leading to less realistic results. Secondly, the changing of the beam distances when done manually along with the optimised parameters are very time consuming. If the whole process is automated, the time consumption for the work will be high for the automation in the beginning but will payoff in the long run. More time is need to investigate into this matter in the future.

Since the reference model has not been compared with experimental data more focus should also be directed in the reference model. Is it correct to use a reference model of a current model system in LS-Dyna or should there actually be physical data to compare with?

Bibliography

Articles

[1] Sandberg H. Rydholm O. (2016) Evaluation of Material Models to Predict Material Failure in LS-DYNA. M.Sc. Lund University.

[2] Faruque O. Saha N. Mallela K. Tyan T. Madasamy C. (2006) Modeling of Spot Weld under Impact Loading and Its Effect on Crash Simulation. SAE International published. SAE number 2006-01-0959.

[3] Noman K. (2007) Development of a Universal spot weld model for automotive FEM crash simulations. B.Sc. RMIT University.

[4] Lim J. Ha J. Oh C. (2015) Practical Failure Criterion of Spot Weld for Crash Simulation. LS-DYNA Conference, Würzburg Germany.

[5] Koralla S. Gadekar G. Nadella P. Dey S. (2015) Spot Weld Failure Prediction in Safety Simulations Using MAT-240 Material Model in LS-DYNA. SAE International published. SAE number 2015-26-0165.

[6] Bier M. Liebold C. Haufe A. Klamser H. (2015) Evaluation of a Rate-Dependent, Elasto-Plastic Cohesive Zone Mixed-Mode Constitutive Model for Spot weld Modeling. LS-DYNA published in Bamberg, Germany.

[7] Hernandez V. Panda S. Okita Y. Zhou N. (2009) A study on heat affected zone softening in resistance spot welded dual phase steel by nanoindentation. Springer published. Article at University of Waterloo, Canada.

[8] Kumagai K. Hayashi S. Ohno Takahiro (2007) Rupture Modeling of Spot Welds under Dynamic Loading for Car Crash FE Analysis. LS-DYNA published in Frankenthal, Germany.

[9] Malcolm S. Nutwell E. (2007) Spotweld Failure Prediction using Solid Element Assemblies. 6th European LS-Dyna published.

Book

[10] Ottosen N. Petersson H. (1992) Introduction to finite element method. University of Lund, Sweden.

Sources without author(s)

[11] BETA CAE Systems SA (2015). ANSA User's Guide.

[12] Livermore Software Technology Corporation (2013). LS-DYNA Keyword User's Manual Volume II, Version R7.0.

Internet sources

[13] FKG. Fordonsindustrin. http://www.fkg.se/fordonsindustrin (Acc 2017-02-21)
[14] Trafikverket. Nollvisionen. https://www.trafikverket.se/om-oss/var-verksamhet/sa-har-jobbar-vi-med/Vart-trafiksakerhetsarbete/Trafiksakerhetsmal/Nollvisionen/ (Acc 2017-02-17)
[15] MATFEM. MF GenYld + CrachFEM. http://www.matfem.de/en/crachfem.html (Acc 2017-03-05)
[16] Weld symbols. Spot weld. https://mechanisttimes.blogspot.se/2014/04/weld-symbols-used-in-design.html (Acc 2017-02-22)
[17] I-Car. Spot weld failure. https://www.i-car.com/graphics/about_icar/current_events/advantage/2007/Advantage_online_1220/full_size/fig_03.jpg (Acc 2017-03-01)
[18] LS-Dyna Support. Shell Formulation. http://www.dynasupport.com/howtos/element/shell-formulations (Acc 2017-02-15)

A

Reference model

The curves along with the failure for respective coupon test are presented in Figure A.1-A.6. These results were baselines for the methods used in the project.

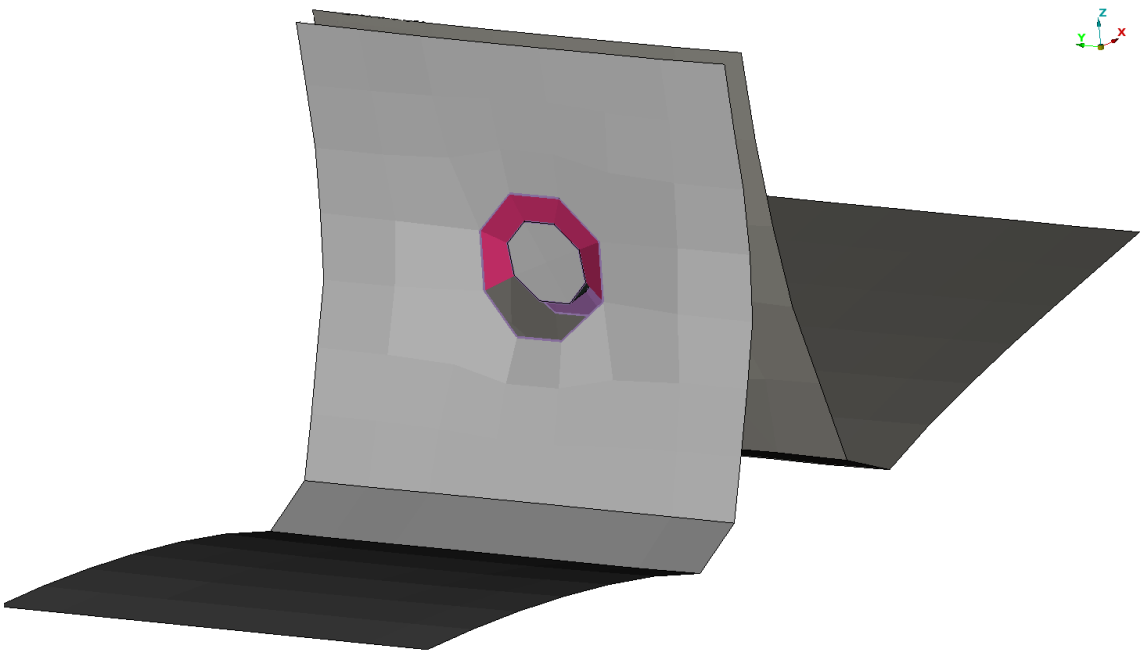

Figure A.1: Failure of the peel test where the HAZ breaks.

The failure of the peel test occurs at 7.5 ms and 3.5 kN, see Figure A.2.

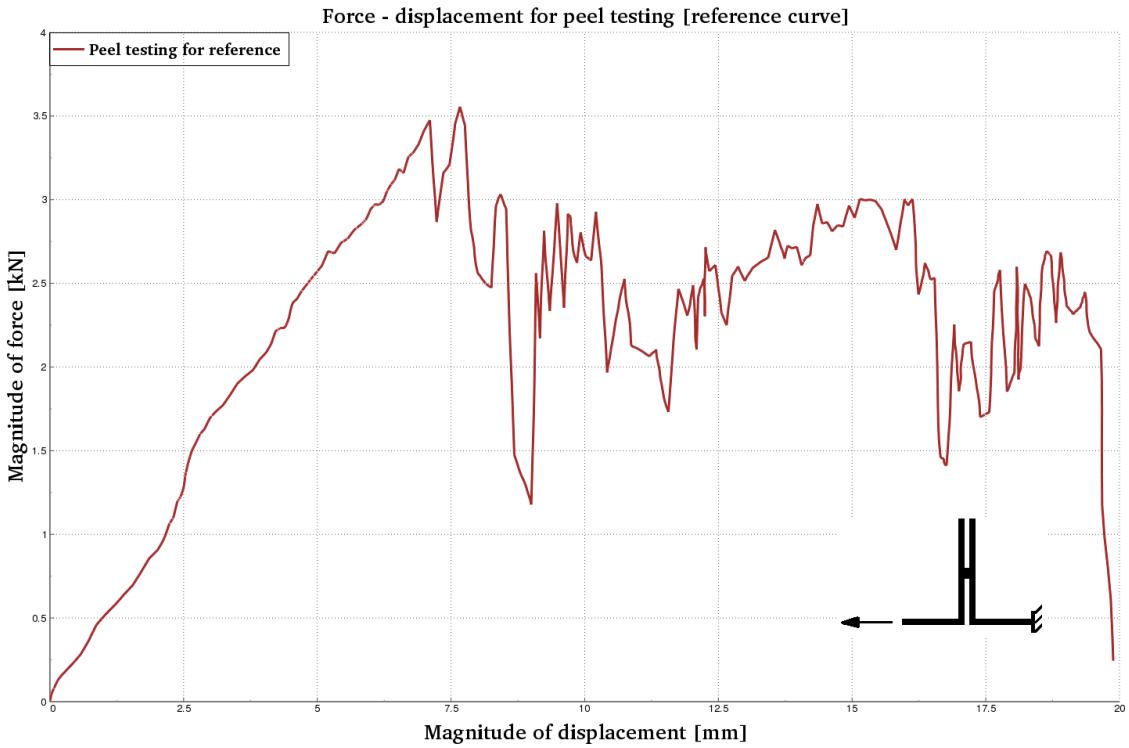

Figure A.2: The reference curve for peeling.

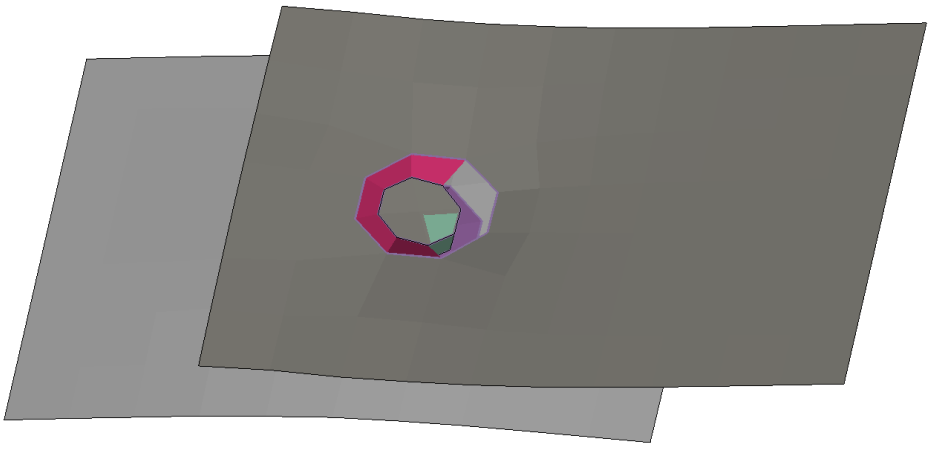

Figure A.3: Failure of the shear test where the HAZ breaks.

The failure of the shear test occurs at 0.5 ms and 20.8 kN, see Figure A.4.

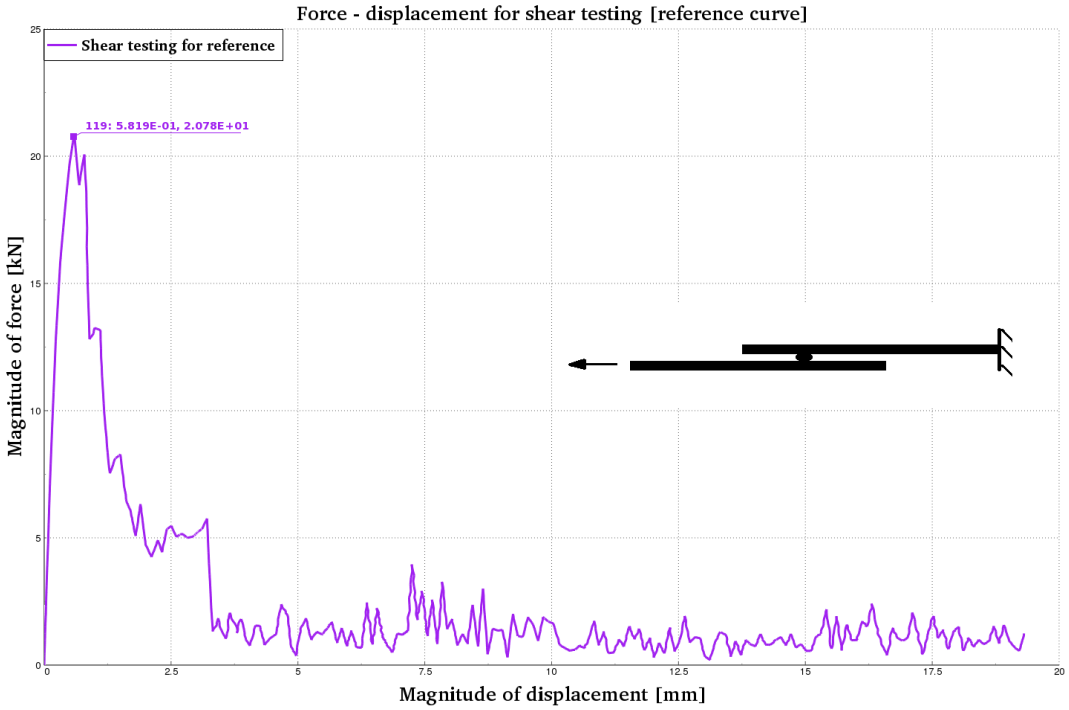

Figure A.4: The reference curve for lap-shear.

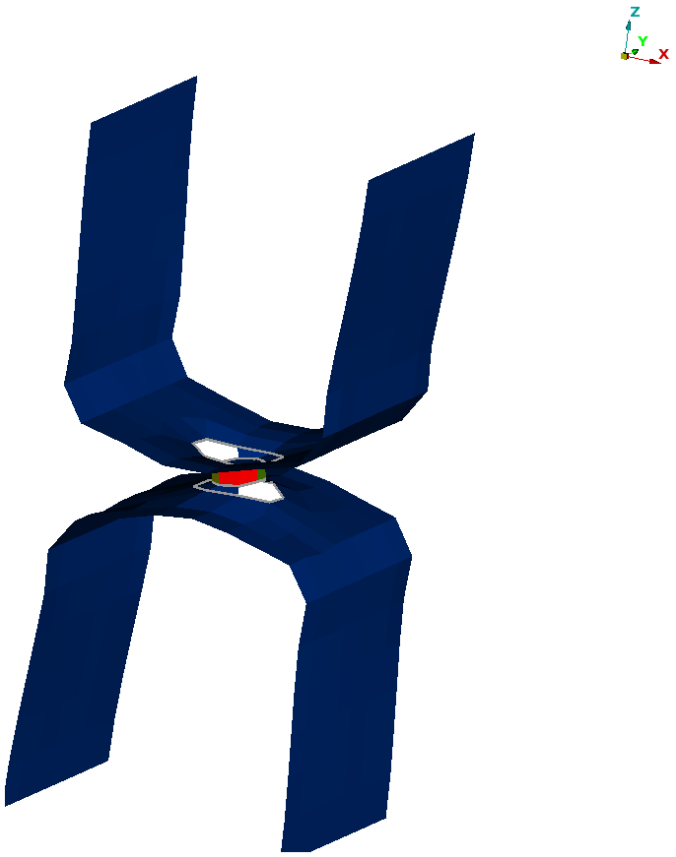

Figure A.5: Failure of the utension test where the HAZ breaks.

The failure of the utension test occurs at 6.8 ms and 11.4 kN, see Figure A.6.

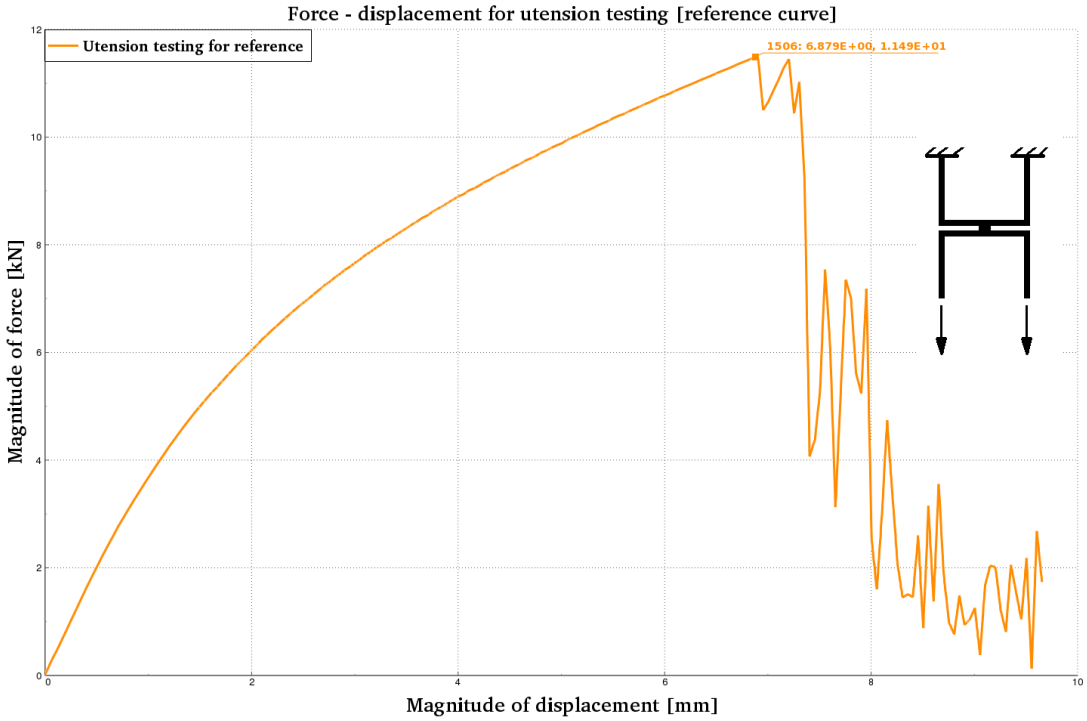

Figure A.6: The reference curve for u-tension.

B

LS-DYNA version

Running the identical setup but with different LS-DYNA versions, from LS-DYNA V971 R6.1.2 (R6.85274) to LS-DYNA R8.1.0 (R8.105341). There were 10 setups of shear simulations and 10 peel simulations which were run in both of the versions. The results were varying within 0-10% in max force, where the later version was failing earlier with lower force values. The difference in time and displacement was up to 5%. Figure B.1 shows one example of the peel test failing earlier for the later version. Figure B.2 shows again where the later version of LS-DYNA fails earlier. Worth mentiong is that the failure mechanics were the same but the failures occured at different displacements and forces.

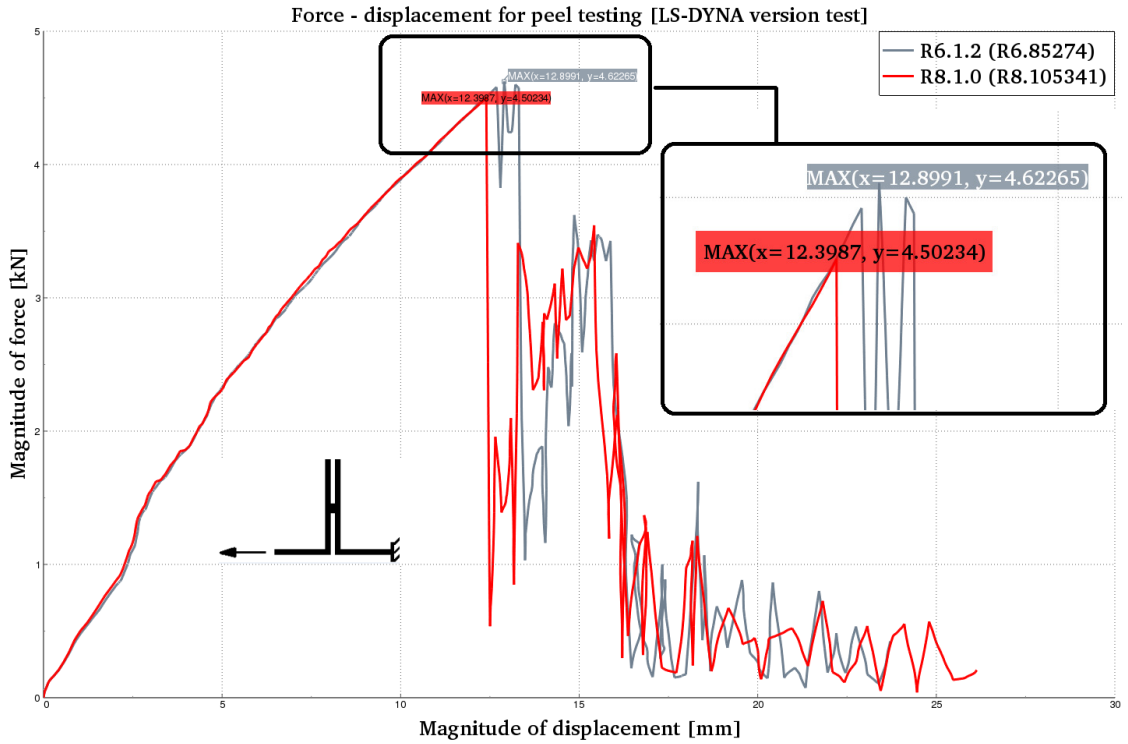

Figure B.1: An example of the later version of LS-DYNA where it fails earlier for peel test.

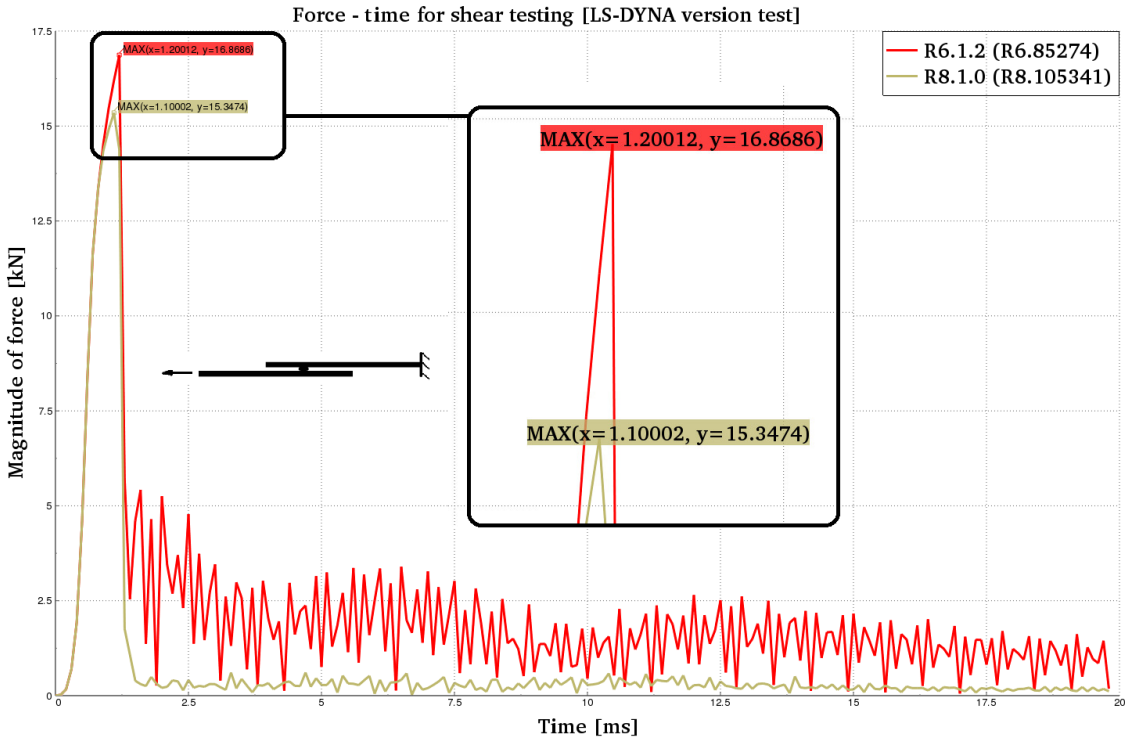

Figure B.2: Another example of the difference between the LS-DYNA version.

If there is going to be further work done on this project one must also consider the LS-Dyna version since the results are not the same between the versions for coupon tests. Re-creating the setup here in wrong version might not lead to the same results.

C

Simulation specimens

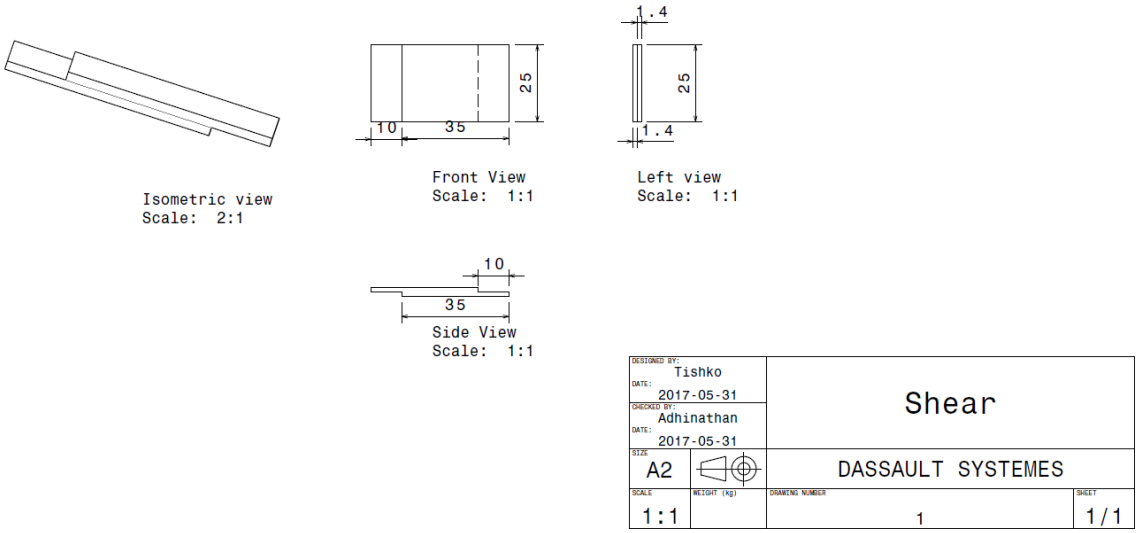

Figure C.1: The geometry shown is for testing of shear specimen.

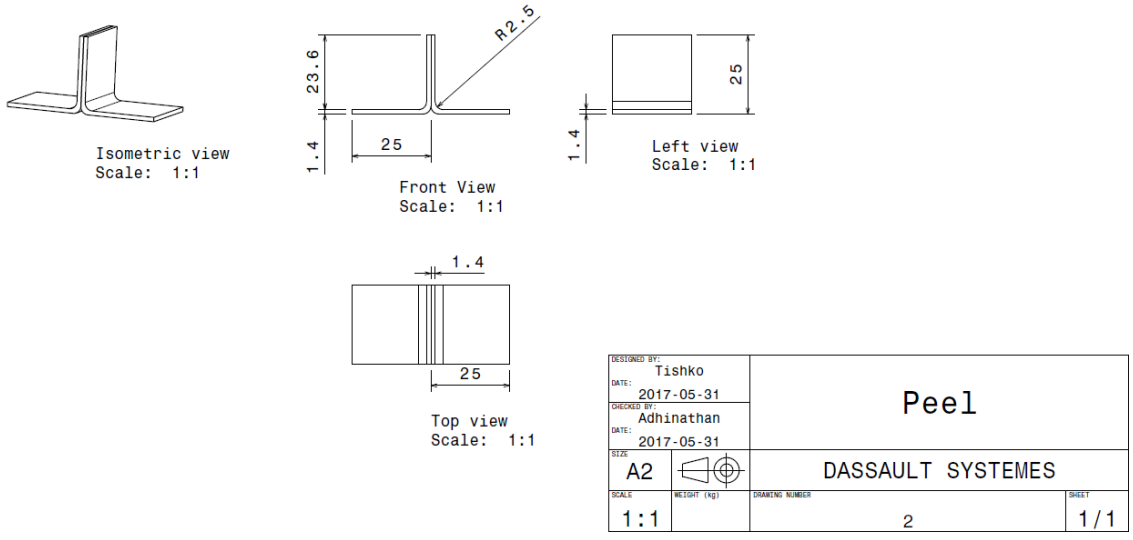

Figure C.2: The geometry shown is for testing of peel specimen.

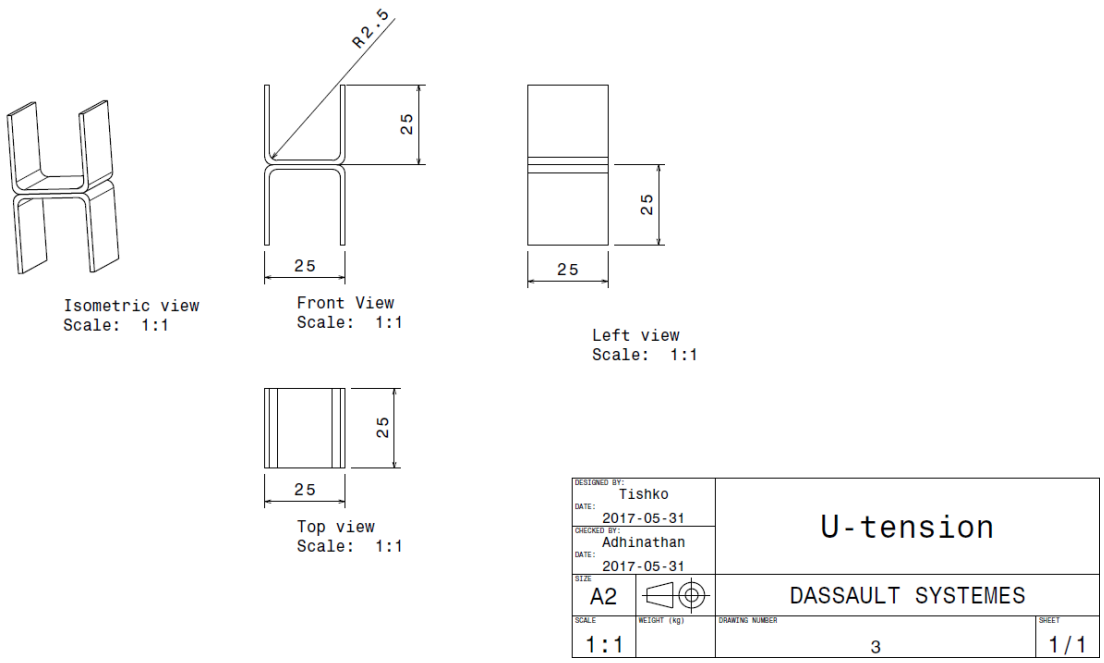

Figure C.3: The geometry shown is for testing of u-tension specimen.